AD-A117 944 OKLAHOMA UNIV NORMAN SCHOOL OF AEROSPACE MECHANICAL --ETC F/G 13/13
ANALYSES OF BEAMS CONSTRUCTED OF NONLINEAR MATERIALS HAVING DIF--ETC(U)
JUL 82 C W BERT, F GORDANINEJAD N00014-78-C-0647
UNCLASSIFIED OU-AMNE-82-5 NL

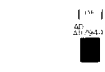

END
DATE FILMED
9 82
DTIC

AD A117 [illegible]

Department of the Navy
OFFICE OF NAVAL RESEARCH
Mechanics Division
Arlington, Virginia 22217

Contract N00014-78-C-0647
Project NR 064-609
Technical Report No. 30

Report OU-AMNE-82-5

ANALYSES OF BEAMS CONSTRUCTED OF NONLINEAR MATERIALS HAVING DIFFERENT BEHAVIOR IN TENSION AND COMPRESSION

by

C.W. Bert and F. Gordaninejad

July 1982

DTIC
ELECTE
AUG 0 6 1982
E

DTIC FILE COPY

School of Aerospace, Mechanical and Nuclear Engineering
University of Oklahoma
Norman, Oklahoma 73019

Approved for public release; distribution unlimited

82 08 06 010

PART I

DEFLECTION OF THICK BEAMS OF MULTIMODULAR MATERIALS

C.W. Bert[+] and F. Gordaninejad[*]
The University of Oklahoma, Norman, Oklahoma, USA 73019

SUMMARY

A transfer-matrix analysis is presented for determining the static behavior of thick beams of "multimodular materials" (i.e., materials which have different elastic behavior in tension and compression, with nonlinear stress-strain curves approximated as piecewise linear, with four or more segments). To validate the transfer-matrix method results, a closed-form solution is also presented for cases in which the neutral-surface location is constant along the beam axis. Numerical results for axial displacement, transverse deflection, bending slope, bending moment, transverse shear, axial force, and location of neutral surface are presented for multimodular and bimodular models of unidirectional aramid cord-rubber. The transfer-matrix method results agree very well with the closed-form solutions.

INTRODUCTION

In 1941 Timoshenko[1] considered the flexural stresses in bimodular material, i.e., a bilinear material having different moduli in tension and in compression. Ambartsumyan[2] in 1965, introduced the terminology, "bimodulus", and extended the concept to two-dimensional materials. Numerous static papers appeared after this work; Marin[3] gave the effective modulus for stiffness

---

[+]Perkinson Professor of Engineering.
*Graduate Research Assistant.

DTIC COPY INSPECTED

For
I
Justification
By
Distribution/
Availability Codes
Dist | Avail and/or Special
A

of bimodular beam undergoing pure bending.

Small-deflection bending of Bernoulli-Euler beams of homogeneous, bimodular material was treated in References 4-12. Large static deflections of beams of bimodular material were analyzed in References 13-14. Kamiya[15] considered transverse-shear-deformation effects on bimodular beams for the first time. Recently Tran and Bert[16] treated bending of thick beams of bimodular materials and obtained both closed-form and transfer-matrix solutions. To the best of the present authors' knowledge, no previous work is available in the context of multimodular beams.

MODELING OF THE STRESS-STRAIN CURVE

Bert and Kumar[17] recently presented experimental stress-strain curves for unidirectional cord-rubber materials. In the present work a stress-strain curve for aramid-rubber taken from [17] has been linearly approximated by four segments (two segments in tension and two segments in compression). For choosing the 'break points' t and c (see Fig. 1) the area between two fitting lines and the experimental curve in each portion has been minimized (see Appendix A). To find comparable moduli for the bimodular case, one has to minimize the area between two straight lines and the experimental curve (also see Appendix A).

THEORY AND FORMULATION

Consider a rectangular-cross-section beam of thickness h and length ℓ as shown in Fig. 2. The origin of the Cartesian coordinate system is located on the mid-surface of the beam with the z-axis being measured positive downward.

1. Displacement Field

The same displacement field used in classical Timoshenko beam theory is implemented here

$$U(x,z) = u(x) + z\psi(x) \quad , \quad W(x,z) = w(x) \tag{1}$$

where U and W are displacements in the x and z directions, respectively, u and w are corresponding displacements at the midplane, and ψ is the bending slope.

2. Stress Field

For a four-segment approximation of the normal stress-strain curve, considering the general case (i.e., when $-\frac{h}{2} < a_c \ , \ a_t < \frac{h}{2}$), the following stress field has been considered for the case of convex bending (see Figs. 1 and 3).

$$\sigma_x \equiv \begin{cases} E_1^c \varepsilon_1^c + E_2^c(\varepsilon_x - \varepsilon_1^c) & -h/2 \le z \le a_c \\ E_1^c \varepsilon_x & a_c \le z \le z_n \\ E_1^t \varepsilon_x & z_n \le z \le a_t \\ E_1^t \varepsilon_1^t + E_2^t(\varepsilon_x - \varepsilon_1^t) & a_t \le z \le h/2 \end{cases} \tag{2}$$

$$\tau_{xz} = G\gamma_{xz}$$

where E_1^c, E_2^c, E_1^t, E_2^t, G, ε_1^c, and ε_1^t are material constants, σ_x is the axial normal stress, ε_x is the axial normal strain, γ_{xz} is the transverse shear strain, τ_{xz} is the transverse shear stress, and z_n is the location of the neutral surface. It is noted that this material is linear elastic in shear. Comparison of Figs. 1 and 3 leads to

$$\varepsilon_x = \kappa(z - z_n) \tag{3}$$

$$\varepsilon_1^c = \kappa(a_c - z_n) \tag{4}$$

$$\varepsilon_1^{\,t} = \kappa(a_t - z_n) \tag{5}$$
$$\varepsilon_f^{\,c} = \kappa(-h/2 - z_n) \tag{6}$$
$$\varepsilon_f^{\,t} = \kappa(h/2 - z_n) \tag{7}$$

where $\varepsilon_f^{\,c}$ and $\varepsilon_f^{\,t}$ are the final values attained at the respective compressive and tensile outer fibers and κ is the curvature.

Using linear strain measure and the strain field of equations (1), one obtains

$$\begin{aligned} \varepsilon_x &= U_{,x} = u_{,x} + z\psi_{,x} = \varepsilon^o + z\psi_{,x} \\ \gamma_{xz} &= W_{,x} + U_{,z} = w_{,x} + \psi \end{aligned} \tag{8}$$

Comparison of equations (3) and (8) gives

$$u_{,x} = -\kappa z_n \quad , \quad \psi_{,x} = \kappa \tag{9}$$

Note that $(\ )_{,x}$ denotes $d(\ )/dx$.

3. Constitutive Relation

For the assumed beam, the normal and transverse shear stress resultants and moment, each per unit width, are defined as

$$(N,Q) = \int_{-h/2}^{h/2} (\sigma_x, \tau_{xz})dz \quad , \quad M = \int_{-h/2}^{h/2} z\sigma_x dz \tag{10}$$

Using the assumed stress and displacement field system of equations (10) can be written as the constitutive relation for a multimodular beam:

$$\begin{Bmatrix} N \\ M \\ Q \end{Bmatrix} = \begin{bmatrix} A + C_N^A & B + C_N^B & 0 \\ B + C_M^B & D + C_M^D & 0 \\ 0 & 0 & S \end{bmatrix} \begin{Bmatrix} u_{,x} \\ \psi_{,x} \\ w_{,x} + \psi \end{Bmatrix} \tag{11}$$

where A, B, D, and S denote the respective extensional, flexural-extensional coupling, flexural, and transverse shear stiffnesses defined by

$$(A,B,D) = \int_{-h/2}^{h/2} (1,z,z^2) E_i^{(k)} dz \qquad \begin{matrix} i=1,2 \\ k=t,c \end{matrix}$$

$$S = K^2 \int_{-h/2}^{h/2} G \, dz \tag{12}$$

Here, the stiffnesses C_N^A, C_N^B, C_M^B, and C_M^D are not present in linear or bimodular materials, and are as defined in Appendix B. In equation (12) t and c denote tensile-strain and compressive-strain regions, respectively. The quantity K^2 is a shear correction coefficient which is generally taken to be 5/6 for static loading of a rectangular-section beam.

4. Equilibrium Equations

The equilibrium equations for transverse distributed loading q(x) can be written as

$$N_{,x} = 0 \quad ; \quad Q_{,x} + q(x) = 0 \quad ; \quad M_{,x} - Q = 0 \tag{13}$$

By substitution of equation (11) into equations (13), one obtains the following equations of equilibrium in terms of the generalized displacements

$$\begin{aligned} &(A'u_{,x} + B'\psi_{,x})_{,x} = 0 \\ &[S(w_{,x} + \psi)]_{,x} = -q(x) \\ &(B''u_{,x} + D'\psi_{,x})_{,x} - S(w_{,x} + \psi) = 0 \end{aligned} \tag{14}$$

where

$$
\begin{aligned}
A' &= A + C_N^A \\
B' &= B + C_N^B \\
B'' &= B + C_M^B \\
D' &= D + C_M^D
\end{aligned}
\tag{15}
$$

CLOSED-FORM SOLUTION

A closed-form solution can be obtained only when the stiffnesses and thus neutral-surface position (z_n) do not depend on x. Therefore, neutral-surface location [18] must be constant

$$z_n = -u_{,x}/\psi_{,x} = \text{constant} \tag{16}$$

Using equation (11) one is able to express $u_{,x}$ and $\psi_{,x}$ in terms of N, M, and the stiffnesses as follows:

$$
\begin{Bmatrix} u_{,x} \\ \psi_{,x} \end{Bmatrix} = \frac{1}{B'B'' - A'D'} \begin{bmatrix} -D' & B' \\ B'' & -A' \end{bmatrix} \begin{Bmatrix} N \\ M \end{Bmatrix} \tag{17}
$$

Combining equations (16) and (17), one obtains

$$z_n = (B'M - D'N)/(A'M - B''N) \tag{18}$$

It is obvious that z_n = const. when N = 0. Thus, for these special cases (see Appendix C)

$$z_n = B'/A' = \text{constant} \tag{19}$$

Now, equilibrium equations (14) can be simplified as follows [19]:

$$
\begin{aligned}
A'u_{,xx} + B'\psi_{,xx} &= 0 \\
S(w_{,xx} + \psi_{,x}) &= -q(x) \\
B''u_{,xx} + D'\psi_{,xx} - S(w_{,x} + \psi) &= 0
\end{aligned}
\tag{20}
$$

The general solution for equations (20) can be written as follows:

$$u(x) = d_1 + d_2 x + \frac{3B'}{A'} C_4 x^2 + u_p(x)$$

$$\psi(x) = -C_2 + \frac{6(B'B''-A'D')}{SA'} C_4 - 2C_3 x - 3C_4 x^2 + \psi_p(x) \qquad (21)$$

$$w(x) = C_1 + C_2 x + C_3 x^2 + C_4 x^3 + w_p(x)$$

where u_p, ψ_p, w_p are particular solutions (see Appendix D) and C_1, C_2, C_3, C_4, d_1, and d_2 are arbitrary constants determined by the boundary conditions of the beam. The following boundary conditions have been considered for closed-form solutions:

1. Hinged-Hinged (free to move axially at x = L)

   $u(0) = N(\ell) = 0 \quad ; \quad M(0) = M(\ell) = 0 \quad ; \quad w(0) = w(\ell) = 0$

2. Clamped-Free

   $u(0) = N(\ell) = 0 \quad ; \quad \psi(0) = M(\ell) = 0 \quad ; \quad w(0) = Q(\ell) = 0$

3. Clamped-Clamped (free to move axially at x = L)

   $u(0) = N(\ell) = 0 \quad ; \quad \psi(0) = \psi(\ell) = 0 \quad ; \quad w(0) = w(\ell) = 0$

The values of constants C_1, C_2, C_3, C_4, d_1, and d_2 are listed in Appendix D.

TRANSFER-MATRIX SOLUTION

As it has been shown in [20,21], in the transfer-matrix approach, the beam is divided into N_s elements, each of which is assumed to be of mass m and concentrated at the center of mass of the element. The mass center of each element is called the station. The stations are separated by fields which are taken to be massless and contain all of the stiffnesses of the beam. At the end points of the beam there are two half fields of length $\ell/2$ (see

Fig. 4), and between these half fields there are N_s stations separated by $(N_s - 1)$ full fields of length, $\Delta\ell$, where $\Delta\ell = \ell/N_s$ and ℓ is the length of the beam. By writing the equilibrium equations for each station and each element and connecting the elements by transfer matrices, one transfers the generalized displacements (u,w,ψ) and the forces (N,Q,M) from the left side of the beam to the right side.

Since the same procedure used in [16] has been used here to derive transfer matrices and state vectors $(u,w,\psi,N,Q,M)^T$, the readers are referred to this reference. Note that since the present work deals with multimodular material, some changes in the field matrix are necessary (see Appendix E). In the calculation of the stiffnesses for the cases where the axial force is not zero, the neutral-surface locations and the corresponding distances to the "break points" in the σ_x vs z curve (a_c and a_t) are not constant and not known a-priori. Therefore, an iterative technique has been employed to compute the neutral-surface locations z_n, also a_c and a_t. One must first assume $(2N_s + 2)$ sets of values of z_n, a_c, and a_t and then compute the stiffnesses and solve the governing equations for the state vector. Finally, by using equations (18), (C.3), and (C.4), compute new values of z_n, a_c, and a_t. Obviously, if the assumed and computed sets of z_n, a_c, and a_t are in sufficiently close agreement, the problem is solved; otherwise, assume the calculated set z_n, a_c, and a_t and repeat the procedure.

NUMERICAL RESULTS

In the following, numerical results are presented for a thick beam with a rectangular cross section and constructed of multimodular material (see Table 1): unidirectional aramid cord-rubber, which is used in the tire

industry. Various boundary conditions and loading conditions were investigated (see Tables 2 and 3). In the transfer-matrix analysis, twenty-five elements were used. Each element was of length 0.32 in. for dimensional cases and dimensionless length of 0.04 for nondimensional cases. The shear correction coefficient was taken to be 5/6.

For all cases considered, the computations are carried out for axial elongation u (or $\bar{u} = u E_2^t/q_o \ell$), transverse deflection W (or $\bar{W} = W E_2^t/q_o \ell$), bending slope ψ (or $\bar{\psi} = \psi E_2^t/q_o$) axial force N (or $\bar{N} = N/q_o \ell$), shear force Q (or $\bar{Q} = Q/q_o \ell$), bending moment M (or $\bar{M} = M/q_o \ell^2$) and neutral-surface location z_n (or $\bar{z}_n = z_n/h$), where $\bar{u}$, $\bar{W}$, $\bar{\psi}$, $\bar{N}$, $\bar{Q}$, $\bar{M}$, and $\bar{z}_n$ are nondimensional parameters.

Due to lack of comparable results in the literature, comparisons are made between the closed-form solution (CFS) and the transfer-matrix solution (TMS) developed here. Excellent agreement between CFS and TMS for the twenty-five element model has been achieved and still it can be improved by increasing the number of elements. For most of the results, the error is less than 2%. Figure 5 contains the plots of the dimensionless transverse deflection ($\bar{W}$) versus dimensionless position ($\bar{X} = x/\ell$) for Case 11 for multimodular, bimodular, unimodular, and average-modular [i.e., $E = (E_b^t + E_b^c)/2$] cases, where $\ell/h = 10$.

As one can see, there is a considerable difference between transverse deflection of multimodular and bimodular models on one hand and unimodular and average modular models on the other. Note that Case 11 is a special case because both ends are not free to move and one expects axial force to be developed due to bending-stretching coupling caused by bimodular action. However, the computed axial force is close to zero which means z_n is constant.

To validate TMS, in Figs. 6 through 9, a comparison is made between TMS and CFS. Behavior of Cases 1, 4, 10, and 11 was studied for the multimodular model considering different dimensionless parameters (ℓ/h = 5, 10, 15, $\bar{M}_1$ = - 1.0, $\bar{N}_1$ = - 1.0, $\bar{Q}_1$ = - 1.0).

In Table 4, for a specific beam (see Table 1), dimensioned comparisons have been made between multimodular and bimodular models. Tables 5, 6, 7 and 9 again show the validity of TMS while they present the computed resu for Cases 3, 5, 6, 7, and 8.

Since closed-form solutions are not available for the complicated boundary conditions considered in Cases 9, 10, and 11, only transfer-matrix results are presented for these cases. In Figs. 10-13 the behavior of a clamped-free beam (with applied moment and axial and shear forces at the free end) and a clamped-clamped beam under a uniform load is investigated. See also Table 10. It is of particular interest to note that in Fig. 10, the sign of the deflection depends upon the ℓ/h ratio, the crossover point being at $\ell/h \simeq 11$.

For cases where axial force is zero, the neutral-surface location is constant; otherwise it varies along the beam length. In Figs. 14-17 the shapes of neutral-surface curves for multimodular and bimodular models have been shown for several cases.

CONCLUSIONS

Analyses of the bending deflection of multimodular thick beams with rectangular cross section based on shear-deformable-beam theory are presented. In this study, both dimensionless and dimensioned results of transfer-matrix, as well as closed-form, solutions for a rectangular multimodular beam of aramid-cord rubber are presented. The transfer-matrix and the closed-form solutions are found to agree very well.

Results of analysis of bimodular and multimodular models show that there is not a drastic difference between the two models. Although the multimodular model is a better one for approximating the stress-strain curve, the bimodular approximation is less complicated. Closed-form solutions are available only for a number of loading/boundary conditions (in which the axial force is identically zero), but the transfer-matrix method can be applied to more complicated geometry, loading, and boundary conditions. In this work, results for several boundary and loading conditions are investigated. The transfer-matrix method is found to be very effective in terms of computational time and also gives results which agree quite well with the closed-form solutions.

ACKNOWLEDGMENTS

The authors gratefully acknowledge the financial support of the Office of Naval Research, Mechanics Division, and the encouragement of Drs. N. Basdekas and Y. Rajapakse. The computing time provided by the University's Merrick Computing Center is also acknowledged.

REFERENCES

1. S. Timoshenko, *Strength of Materials*, Pt. II: Advanced Theory and Problems, 2nd. ed., Van Nostrand, Princeton, NJ, pp. 362-369, 1941.

2. S.A. Ambartsymyan, 'The axisymmetric problem of a circular cylindrical shell made of material with different stiffnesses in tension and compression', *Izvestiya Akademiya Nauk SSSR, Mekhanika*, no. 4, 77-85 (1965); Engl. trans., National Tech. Information Center Document AD-675321 (1967).

3. J. Marin, *Mechanical Behavior of Engineering Materials*, Prentice-Hall, Englewood Cliffs, NJ, pp. 86-88, 1962.

4. A.A. Shlyakhman and V.A. Lepetov, 'Calculations of hose for bending. 2. Determining the radius of curvature of the longitudinal axis of hose in bending, taking into account the displacement of neutral surface', *Soviet Rubber Technology*, 18(8), 50-54 (Aug. 1959).

5. E.F. Rybicki and M.F. Kanninen, 'The effect of different behavior in tension than in compression on the mechanical response of polymeric materials', *Deformation and Fracture of High Polymers* (Battelle Institute Science Colloquium, Kronberg, Germany, Sept. 11-16, 1972), H.H. Kausch, J.H. Hassel, and R.I. Jaffee, Plenum, New York, pp. 417-427, 1973.

6. S.G. Sterling, 'The flexural behavior of thermoplastic beams', *Plastics and Polymers* 40, 228-235 (1972).

7. A. Simkin and G. Robin, 'The mechanical testing of bone in bending', *Journal of Biomechanics* 6, 31-39 (1973).

8. J.G. Williams, 'Different moduli in tension and compression', *Stress Analysis of Polymers*, Longman, London, pp. 124-126, 1973.

9. F. Tabaddor, 'Analysis for beams made of bi-modulus elastic orthotropic materials', *Fibre Science and Technology* 9, 51-62 (1967).

10. A.G. Goloyan and A.A. Khachatryan, 'Bending of beams made of material with different moduli in tension and compression (in Russian)', *Doklady Akademiya Nauk Armyanskoi SSR* 62, 151-157 (1967). See *Applied Mechanics Reviews* 32, Rev. 190 (1979).

11. V.E. Starzhinskii and V.V. Mozharovskii, 'Determination of the maximum stresses in a cantilever, composed of material with deformation anisotropy, *Polymer Mechanics* 12, 400-405 (1967).

12. T.H. Topper, A.N. Sherbourne, and V. Saari, 'Bending of glass fibre-reinforced plastic (GFRP) plates on elastic supports, Part I: Material characteristics, *Materials and Structures* 11(62), 75-91 (1978).

13. N. Kamiya, 'A refined strain energy formulation for bimodulus material and its application to non-linear bending of a beam,' *Transactions, Japan Society for Composite Materials* 1, 10-16 (1976).

14. S.G. Paolineiis, S.A. Paipetis, and P.S. Theocaris, 'Three-point bending at large deflections of beams with different moduli of elasticity in tension and compression', *Journal of Testing and Evaluation* 7, 177-182 (1979).

15. N. Kamiya, "Transverse shear effect in a bimodulus plate', *Nuclear Engineering and Design* 32, 351-357 (1975).

16. A.D. Tran and C.W. Bert, 'Bending of thick beams of bimodulus materials,' *Computers and Structures* (to appear, 1982).

17. M. Kumar and C.W. Bert, 'Experimental characterization of material behavior of cord-rubber composites,' Proc., First Tire Science and Technology Conference, Akron, OH, March 25-26, 1982.

18. C.W. Bert, J.N. Reddy, V.S. Reddy, and W.C. Chao, 'Bending of thick rectangular plates laminated of bimodulus composite materials,' *AIAA Journal* 19, 1342-1349 (1981).

19. Y.R. Kan and Y.M. Ito, 'Shear deformation in heterogeneous anisotropic plates', *Journal of Composite Materials* 6, 316-319 (1972).

20. E.C. Pestel and F.A. Leckie, *Matrix Methods in Elastomechanics*, Van Nostrand, Princeton, NJ, pp. 51-94, 1963.

21. L. Meirovitch, *Analytical Methods in Vibrations*, Macmillan, New York, pp. 251-262, 1967.

22. B. Carnahan, H.A. Luther, and J.O. Wilkes, *Applied Numerical Methods*, John Wiley and Sons, New York, pp. 308-309, 1969.

APPENDIX A

FITTING MINIMIZED CURVES TO THE STRESS-STRAIN CURVE

1. Multimodular Case

Consider the nonlinear stress-strain curve shown in Fig. A.1. For any arbitrary point (ε^t,σ^t) in the tension region ($\varepsilon \geq 0$), there are two straight lines such that

$$g(\varepsilon) \equiv \begin{cases} (\sigma^t/\varepsilon^t)\varepsilon \\ [(\sigma^t - \sigma_f{}^t)/(\varepsilon^t - \varepsilon_f{}^t)](\varepsilon - \varepsilon_f{}^t) + \sigma_f{}^t \end{cases} \tag{A.1}$$

The equation of a stress-strain curve as expressed in [17] is

$$\sigma(\varepsilon) = K\varepsilon^n \quad ; \quad \varepsilon \geq 0 \tag{A.2}$$

where K and n are constants depending on the material. To find the proper "break point" (ε^t,σ^t), the area between the approximated curve $g(\varepsilon)$ and the actual experimental curve $\sigma(\varepsilon)$ has to be minimized. The mentioned area can be expressed

$$A = \left| \int_0^{\varepsilon^t} [g_1(\varepsilon) - \sigma(\varepsilon)]d\varepsilon \right| + \left| \int_{\varepsilon^t}^{\varepsilon_f^t} [g_2(\varepsilon) - \sigma(\varepsilon)]d\varepsilon \right| \tag{A.3}$$

Substitution of equations (A.1) and (A.2) into equation (A.3) and taking the integrations gives

$$A = \left| \frac{1}{2}\sigma^t\varepsilon^t - \frac{K}{n+1}(\varepsilon^t)^{n+1} \right| + \left| \frac{1}{2}(\sigma_f{}^t + \sigma^t)(\varepsilon_f{}^t - \varepsilon^t) - \frac{K}{n+1}[(\varepsilon_f{}^t)^{n+1} - (\varepsilon^t)^{n+1}] \right| \tag{A.4}$$

By searching in the region of $\Omega \equiv (0,\varepsilon_t{}^f) \times (0,\sigma_t{}^f)$, one is able to find a point (ε^t,σ^t) such that A is minimized locally. Note that a few other methods (e.g., least-squares method) have been tried but it turned out that

the absolute minimum point was outside of the region Ω.

2. Bimodular Case

For this case, the least-squares method has been used. As shown in Fig. A.2, there is a line such that

$$I = \int_0^{\varepsilon_f^t} [E_b^t \varepsilon - K\varepsilon^n]^2 \, d\varepsilon \tag{A.5}$$

can be minimized in Ω. Here, E_b^t is the slope of that line. By taking the derivative of equation (A.5) and equating it to zero, one has

$$\frac{dI}{dE_b^t} = 2 \int_0^{\varepsilon_f^t} [E_b^t \varepsilon - K\varepsilon^n]\varepsilon \, d\varepsilon = 0 \tag{A.6}$$

By solving equation (A.6) for E_b^t, one obtains

$$E_b^t = \frac{3K}{n+2} (\varepsilon_f^t)^{n-1} \tag{A.7}$$

For example, for aramid-rubber in the tension region (see [17]), the following parameters are found:

$$n_t = 1.22$$

$$K_t = 1.1 \times 10^6 \text{ psi}$$

$$\varepsilon_f^t = 0.029$$

$$E_b^t = \frac{(3)(1.1 \times 10^6)}{1.22 + 2} (0.029)^{1.22-1} = 0.47 \times 10^6 \text{ psi}$$

An analogous calculation can be applied for the compression side of the bend, i.e., E_b^c can be found, provided that K_c, n_c, and ε_f^c are known.

3. Unimodular Case

Using the same method as in Case 2 and assuming only one line, which passes through the origin, to approximate both tension and compression regions (Fig. A.3), one has

$$I = \int_{\varepsilon_f^c}^{0} [K_c \varepsilon^{n_c} - E\varepsilon]^2 d\varepsilon + \int_{0}^{\varepsilon_f^t} [K_t \varepsilon^{n_t} - E\varepsilon]^2 d\varepsilon \tag{A.8}$$

and, then

$$\frac{dI}{dE} = 2\varepsilon[\int_{\varepsilon_f^c}^{0} (K_c \varepsilon^{n_c} - E\varepsilon)\varepsilon \, d\varepsilon + \int_{0}^{\varepsilon_f^t} (K_t \varepsilon^{n_t} - E\varepsilon)\varepsilon \, d\varepsilon] = 0 \tag{A.9}$$

Solving equation (A.9) for E, one obtains

$$E = 2[\frac{K_c}{n_c + 1} (\varepsilon_f^c)^{n_c+1} - \frac{K_t}{n_t + 1} (\varepsilon_f^t)^{n_c+1}]/[(\varepsilon_f^c)^2 - (\varepsilon_f^t)^2] \tag{A.10}$$

NOTE: In the present computations, the values of ε_f^c and ε_f^t considered are as follows:

$$\varepsilon_f^c = 0.046 \quad ; \quad \varepsilon_f^t = 0.029$$

The constants K_c, K_t, n_c, and n_t are listed in [17].

APPENDIX B

THE BEAM STIFFNESSES FOR RECTANGULAR-SECTION BEAMS OF MULTIMODULUAR MATERIALS

For the assumed four-segment model, there are two different bending cases in general, convex downward and concave downward bending. In convex downward bending, the top layer of a beam is in compression and the bottom layer in tension. Conversely, in concave downward bending, the top layer of the beam is in tension and the bottom layer is in compression.

Depending on the location of z_n, a_c, and a_t in ε_x vs z, eight different cases might occur. For example, for convex downward bending, consider the case when z_n, a_c, and a_t are in the range of -h/2 and h/2 (see Fig. 3). Substitution of equation (2) into equation (10) and using equations (3), (4), and (5) leads to

$$N = \int_{-h/2}^{a_c} [\kappa E_1^c(a_c - z_n) + \kappa E_2^c(z - a_c)]dz + \int_{a_c}^{z_n} \kappa E_1^c(z - z_n)dz + \int_{z_n}^{a_t} \kappa E_1^t(z - z_n)dz$$

$$+ \int_{a_t}^{h/2} [\kappa E_1^t(a_t - z_n) + \kappa E_2^t(z - a_t)]dz \qquad (B.1)$$

and

$$M = \int_{-h/2}^{a_c} [\kappa E_1^c(a_c - z_n) + \kappa E_2^c(z - a_c)]z\, dz + \int_{a_c}^{z_n} \kappa E_1^c(z - z_n)z\, dz$$

$$+ \int_{z_n}^{a_t} \kappa E_1^t(z - z_n)z\, dz + \int_{a_t}^{h/2} [\kappa E_1^t(a_t - z_n) + \kappa E_2^t(z - a_t)]z\, dz \qquad (B.2)$$

Equations (B.1) and (B.2) can be written in the following form

$$N = (-\kappa z_n)\{[\int_{-h/2}^{a_c} E_2{}^c dz + \int_{a_c}^{z_n} E_1{}^c dz + \int_{z_n}^{a_t} E_1{}^t dz + \int_{a_t}^{h/2} E_2{}^t dz]$$

$$+ [-\int_{-h/2}^{a_c} E_2 z dz + \int_{-h/2}^{a_c} E_1{}^c dz + \int_{a_t}^{h/2} E_1{}^t dz - \int_{a_t}^{h/2} E_2{}^t dz]\}$$

$$+ (\kappa)\{[\int_{-h/2}^{a_c} E_2{}^c z\, dz + \int_{a_c}^{z_n} E_1{}^c z\, dz + \int_{z_n}^{a_t} E_1{}^t z\, dz + \int_{a_t}^{h/2} E_2{}^t z\, dz]$$

$$+ [\int_{-h/2}^{a_c} E_2{}^c a_c dz - \int_{-h/2}^{a_c} E_1{}^c a_c dz + \int_{a_t}^{h/2} E_1{}^t a_t dz - \int_{a_t}^{h/2} E_2{}^t a_t dz]\} \qquad (B.3)$$

$$M = (-\kappa z_n)\{[\int_{-h/2}^{a_c} E_2{}^c z\, dz + \int_{a_c}^{z_n} E_1{}^c z\, dz + \int_{z_n}^{a_t} E_1{}^t z\, dz + \int_{a_t}^{h/2} E_2{}^t z\, dz]$$

$$+ [-\int_{-h/2}^{a_c} E_2{}^c z\, dz + \int_{-h/2}^{a_c} E_1{}^c z\, dz + \int_{a_t}^{h/2} E_1{}^t z\, dz - \int_{a_t}^{h/2} E_2{}^t z\, dz]$$

$$+ (\kappa)\{[\int_{-h/2}^{a_c} E_2{}^c z^2 dz + \int_{a_c}^{z_n} E_1{}^c z^2 dz + \int_{z_n}^{a_t} E_1{}^t z^2 dz + \int_{a_t}^{h/2} E_2{}^t z^2 dz]$$

$$+ [\int_{-h/2}^{a_c} E_2{}^c a_c dz - \int_{-h/2}^{a_c} E_1{}^c a_c dz + \int_{a_t}^{h/2} E_1{}^t a_t dz - \int_{a_t}^{h/2} E_2{}^t a_t dz]\} \qquad (B.4)$$

Combining equations (9) and (11), one gets

$$N = (-\kappa z_n)A' + \kappa B' \tag{B.5}$$

$$M = (-\kappa z_n)B'' + \kappa D' \tag{B.6}$$

Comparison of equations (B.3) and (B.5) with equations (B.4) and (B.6) and considering equations (12) and (15), one finds that

$$\begin{aligned}
C_A^N &= \int_{-h/2}^{a_c} (E_1^c - E_2^c)dz + \int_{a_t}^{h/2} (E_1^t - E_2^t)dz \\
C_B^N &= \int_{-h/2}^{a_c} (E_2^c - E_1^c)a_c dz + \int_{a_t}^{h/2} (E_1^t - E_2^t)a_t dz \\
C_B^M &= \int_{-h/2}^{a_c} (E_1^c - E_2^c)z\, dz + \int_{a_c}^{h/2} (E_1^t - E_2^t)z\, dz \\
C_D^M &= \int_{-h/2}^{a_c} (E_2^c - E_1^c)a_c z\, dz + \int_{a_c}^{h/2} (E_1^t - E_2^t)a_t z\, dz
\end{aligned} \tag{B.7}$$

As mentioned before, eight cases may occur depending on the location of z_n, a_c, and a_t. These cases have been analyzed as the same as the general case as follows (for convex downward bending)

Case 1:

$$T_x \equiv E_1^t \varepsilon_1^t + E_2^t(\varepsilon_x - \varepsilon_1^t) \qquad -h/2 \le z \le h/2 \tag{B.8}$$

$$\begin{aligned}
A' &= hE_1^t \\
B' &= ha_t(E_1^t - E_2^t) \\
B'' &= 0 \\
D' &= h^3E_2^t/24
\end{aligned} \tag{B.9}$$

Case 2:

$$\sigma_x = \begin{cases} E_1^t \varepsilon_1^t + E_2^t(\varepsilon_x - \varepsilon_1^t) & a_t \le z \le h/2 \\ E_1^t \varepsilon_x & -h/2 \le z \le a_t \end{cases} \tag{B.10}$$

$$\begin{aligned} A' &= hE_1^t \\ B' &= -(E_1^t - E_2^t)(h/2 - a_t)^2/2 \\ B'' &= 0 \\ D' &= [h^3(E_1^t + E_2^t)/8 + a_t^3(E_2^t - E_1^t)/2]/3 + h^2 a_t(E_1^t - E_2^t)/8 \end{aligned} \tag{B.11}$$

Case 3:

$$\sigma_x = \begin{cases} E_1^t \varepsilon_1^t + E_2^t(\varepsilon_x - \varepsilon_1^t) & a_t \le z \le h/2 \\ E_1^t \varepsilon_x & z_n \le z \le a_t \\ E_1^c \varepsilon_x & -h/2 \le z \le z_n \end{cases} \tag{B.11}$$

$$\begin{aligned} A' &= h(E_1^c + E_1^t)/2 + z_n(E_1^c - E_1^t) \\ B' &= [h^2(E_2^t - E_1^c)/2 + a_t(h - a_t)(E_1^t - E_2^t) + z_n^2(E_1^c - E_1^t)]/2 \\ B'' &= (E_1^t - E_1^c)(h^2/4 - z_n^2)/2 \\ D' &= [h^3(E_1^c + E_2^t)/8 + a_t^3(E_2^t - E_1^t)/2 + z_n^3(E_1^c - E_1^t)]/3 \\ &\quad + h^2 a_t(E_1^t - E_2^t)/8 \end{aligned} \tag{B.12}$$

Case 4:

This case is the general case (see Fig. 3) which has been discussed in detail earlier in this Appendix.

Case 5:

$$\sigma_x = \begin{cases} E_1^t \varepsilon_x & z_n \le z \le h/2 \\ E_1^c \varepsilon_x & a_c \le z \le z_n \\ E_1^c \varepsilon_1^c + E_2^c(\varepsilon_x - \varepsilon_1^c) & -h/2 \le z \le a_c \end{cases} \tag{B.13}$$

$$A' = h(E_1^t + E_1^c) + z_n(E_1^c - E_1^t)$$
$$B' = [h^2(E_1^t - E_2^c)/4 + z_n^2(E_1^c - E_1^t) + a_c(a_c + h)(E_1^c - E_2^c)]/2$$
$$B'' = (E_1^t - E_1^c)(h^2/4 - z_n^2)/2 \qquad (B.14)$$
$$D' = [h^3(E_1^t + E_2^c) + z_n^3(E_1^c - E_1^t) + a_c^3(E_1^c - E_2^c)/2]/3 - h^3 a_c(E_1^c - E_2^c)/8$$

Case 6:

$$\sigma_x \equiv \begin{cases} E_1^c \varepsilon_x & a_c \le z \le h/2 \\ E_1^c \varepsilon_1^c + E_2^c(\varepsilon_x - \varepsilon_1^c) & -h/2 \le z \le a_c \end{cases} \qquad (B.15)$$

$$A' = hE_1^c$$
$$B' = (E_1^c - E_2^c)(h/2 + a_c)^2/2$$
$$B'' = 0$$
$$D' = [h^3(E_1^c + E_2^c)/8 + a_c^3(E_1^c - E_2^c)]/3 - h^2 a_c(E_1^c - E_2^c)/8$$

Case 7:

$$\sigma_x \equiv E_1^c \varepsilon_1^c + E_2^c(\varepsilon_x - \varepsilon_1^c) \qquad -h/2 \le z \le h/2 \qquad (B.17)$$

$$A' = hE_1^c$$
$$B' = ha_c(E_1^c - E_2^c) \qquad (B.18)$$
$$B'' = 0$$
$$D' = h^3 E_2^c/24$$

Case 8:

$$\sigma_x \equiv \begin{cases} E_1^t \varepsilon_x & z_n \le z \le h/2 \\ E_1^c \varepsilon_x & -h/2 \le z \le z_n \end{cases} \qquad (B.19)$$

$$
\begin{aligned}
A' &= h(E_1^t + E_1^c) + z_n(E_1^c - E_1^t) \\
B' &= (E_1^t - E_1^c)(h^2/4 - z_n^2)/2 \\
B'' &= (E_1^t - E_1^c)(h^2/4 - z_n^2)/2 \\
D' &= [h^3(E_1^t + E_1^c)/8 + z_n^3(E_1^c - E_1^t)]/3
\end{aligned}
\tag{B.20}
$$

For concave downward bending, one is able to derive similar equations for stiffnesses by converting as follows:

$$
\begin{array}{lll}
E_2^c \longrightarrow E_2^t & E_1^t \longrightarrow E_1^c & a_c \longrightarrow a_t \\
E_1^c \longrightarrow E_1^t & E_2^t \longrightarrow E_2^c & a_t \longrightarrow a_c
\end{array}
$$

APPENDIX C

COMPUTATION OF z_n, a_c, AND a_t

For multimodnular beams, the following equation is not sufficient to determine the neutral-surface location z_n

$$z_n = \frac{B'M - D'N}{A'M - B''N} \tag{C.1}$$

even for cases where N = 0

$$z_n = B'/A' \tag{C.2}$$

Two more equations are needed for computing z_n because the stiffnesses are not only dependent on z_n but they are functions of a_c and a_t as well. Dividing equation (4) by equation (6) and equation (5) by equation (7) and solving for a_c and a_t, one can get (for the convex downward case)

$$a_c = (\varepsilon_1^c/\varepsilon_f^c)\,(h/2 + z_n) - z_n \tag{C.3}$$

$$a_t = (\varepsilon_1^t/\varepsilon_f^t)\,(h/2 - z_n) + z_n \tag{C.4}$$

For the concave downward case

$$a_c = (\varepsilon_1^c/\varepsilon_f^c)\,(h/2 - z_n) + z_n \tag{C.5}$$

$$a_t = (\varepsilon_1^t/\varepsilon_f^t)\,(h/2 + z_n) - z_n \tag{C.6}$$

The system of nonlinear equations (C.1), (C.3), and (C.4) for the convex downward case, or equations (C.1), (C.5), and (C.6) for the concave downward case, can be solved by using iteration of the Gauss-Seidel type [22].

APPENDIX D

ARBITRARY CONSTANTS AND PARTICULAR SOLUTIONS

The values of constants C_1, C_2, C_3, C_4, d_1, and d_2 for the various boundary conditions considered are listed below.

1. Hinged-Hinged (free to move axially at x = L)

$$\begin{aligned}
C_1 &= -u_p(0)\\
C_2 &= -(C_3\ell + C_4\ell^2) - [w_p(\ell) - w_p(0)]/\ell\\
C_3 &= [w_{p,x}(\ell)/2] - 3C_4\ell\\
C_4 &= \frac{A'}{6\ell(A'D' - B'B'')}\,[B'[u_{p,x}(\ell) - u_{p,x}(0)] + D'[w_{p,x}(\ell) - w_{p,x}(0)]]
\end{aligned} \tag{D.1}$$

$$\begin{aligned}
d_1 &= -u_p(0)\\
d_2 &= -[u_{p,x}(\ell) + (6B'/A')C_4\ell]
\end{aligned}$$

2. Clamped-Free

$$\begin{aligned}
C_1 &= -w_p(0)\\
C_2 &= -w_{p,x}(\ell) - w_p(\ell) + w_p(0)\\
C_3 &= w_{p,x}(\ell)/2 + \frac{A'S}{2(B'B'' - A'D')}\,[w_{p,x}(\ell) + w_p(\ell)]\\
C_4 &= \frac{A'S}{6(B'B'' - A'D')}\,[C_2 - w_p(0)]
\end{aligned} \tag{D.2}$$

$$d_1 = - u_p(0)$$

$$d_2 = - u_{p,x}(\ell) + \frac{B'S\ell}{B'B'' - A'D'} [w_{p,x}(\ell) + \psi_p(\ell)]$$

3. Clamped-Clamped (free to move axially at x = L)

$$C_1 = - w_p(0)$$

$$C_2 = \frac{6(B'B'' - A'D')}{SA'} C_4 + \psi_p(0)$$

$$C_3 = [u_p(0) - u_p(\ell) - (3B'/A')C_4\ell^2]/2\ell \qquad (D.3)$$

$$C_4 = \frac{SA'}{SA'\ell^2 - 12(B'B'' - A'D')} [\psi_p(0) + \psi_p(\ell) - 2[w_p(0) - w_p(\ell)]/\ell]$$

$$d_1 = - u_p(0)$$

$$d_2 = [u_p(0) - u_p(\ell) - (3B'/A')C_4\ell^2]/\ell$$

The particular solutions for uniform and sinusoidal normal load are as listed below.

For uniform normal load $q(x) = q_o$:

$$u_p(x) = \frac{B'q_o}{6(A'D' - B'B'')} x^3$$

$$\psi_p(x) = - \frac{q_o}{S} x - \frac{A'q_o}{6(A'D' - B'B'')} x^3 \qquad (D.4)$$

$$w_p(x) = \frac{A'q_o}{24(A'D' - B'B'')} x^4$$

For normal load $q(x) = q_o \sin \alpha x$, where $\alpha \equiv n\pi/\ell$:

$$u_p(x) = \frac{B'q_o}{\alpha^2(A'D' - B'B'')} \cos \alpha x$$

$$\psi_p(x) = - \frac{A'q_o}{\alpha^2(A'D' - B'B'')} \cos \alpha x \qquad (D.5)$$

$$w_p(x) = \frac{q_o}{\alpha^2} [\frac{1}{S} + \frac{A'}{\alpha^2(A'D' - B'B'')} \sin \alpha x]$$

For normal load $q(x) = q_o \cos \alpha x$:

$$u_p(x) = - \frac{B'q_o}{(A'D' - B'B'')} \sin \alpha x$$

$$\psi_p(x) = \frac{A'q_o}{\alpha^3(A'D' - B'B'')} \sin \alpha x \qquad (D.6)$$

$$w_p(x) = \frac{q_o}{\alpha^2} \left[\frac{1}{S} + \frac{A'}{\alpha^2(A'D' - B'B'')}\right] \cos \alpha x$$

APPENDIX E

TRANSFER MATRICES

The equilibrium equations for each station can be written in matrix notation as follows

$$\begin{Bmatrix} U \\ W \\ \psi \\ N \\ Q \\ M \\ 1 \end{Bmatrix}_i^R = \begin{bmatrix} 1 & 0 & 0 & 0 & 0 & 0 & 0 \\ 0 & 1 & 0 & 0 & 0 & 0 & 0 \\ 0 & 0 & 1 & 0 & 0 & 0 & 0 \\ 0 & 0 & 0 & 1 & 0 & 0 & 0 \\ 0 & 0 & 0 & 0 & 1 & 0 & q_s \\ 0 & 0 & 0 & 0 & 0 & 0 & 1 \\ 0 & 0 & 0 & 0 & 0 & 0 & 1 \end{bmatrix}_i \begin{Bmatrix} U \\ W \\ \psi \\ N \\ Q \\ M \\ 1 \end{Bmatrix}_i^L \qquad (E.1)$$

where q_s is the concentrated load at each station. In more compact form equation (E.1) is

$$[S]_i^R = [T_S]_i [S]_i^L \qquad (E.2)$$

The matrix $[T_S]_i$ is known as the station matrix. In matrix notation the equilibrium equation for each field under a distributed load $q(x)$ is

$$\begin{Bmatrix} U \\ W \\ \psi \\ N \\ Q \\ M \\ 1 \end{Bmatrix}_{i+1} = \begin{bmatrix} 1 & 0 & 0 & \frac{B'\Delta\xi}{\gamma} & \frac{B'(\Delta\xi)^2}{2\gamma} & \frac{-D'\Delta\xi}{\gamma} & \frac{-B'\Delta\xi}{2\gamma} K_m \\ 0 & 0 & -\Delta\xi & \frac{A'(\Delta\xi)^2}{2\gamma} & [\frac{\Delta\xi}{S} + \frac{A'(\Delta\xi)^3}{4\gamma}] & \frac{-B'(\Delta\xi)^2}{2\gamma} & \frac{-A'(\Delta\xi)^2}{4\gamma} K_m - \frac{\Delta\xi}{2S} K_q \\ 0 & 0 & 1 & \frac{-A'\Delta\xi}{\gamma} & \frac{-A'(\Delta\xi)^2}{2\gamma} & \frac{B'\Delta\xi}{\gamma} & \frac{A'\Delta\xi}{2\gamma} K_m \\ 0 & 0 & 0 & 1 & 0 & 0 & 0 \\ 0 & 0 & 0 & 0 & 1 & 0 & -K_q \\ 0 & 0 & 0 & 0 & \Delta\xi & 0 & -K_m \\ 0 & 0 & 0 & 0 & 0 & 0 & 1 \end{bmatrix}_i \begin{Bmatrix} U \\ W \\ \psi \\ N \\ Q \\ M \\ 1 \end{Bmatrix}_i \tag{E.3}$$

where

$$\gamma \equiv B'B'' - A'D'$$

$$K_q \equiv \int_0^{\Delta\xi} q(\xi)d\xi \tag{E.4}$$

$$K_m \equiv \int_0^{\Delta\xi} \xi q(\xi)d\xi$$

Values of K_m and K_q for various loadings are listed in Table 2. Equation (E.4) also can be written as

$$[S]^L_{i+1} = [T_j]_i [S]^R_i \tag{E.5}$$

The matrix $[T_j]_i$ is called the field matrix.

Table 1. Elastic Properties and Geometric Parameters for an Aramid-Cord Rubber Beam

Elastic Properties	Longitudinal Young's Modulus, psi x 10^{-6}			Longitudinal-Thickness Shear Modulus, psi x 10^{-3}
	Model*	Tension	Compression	Tension and Compression
	M	E_2^t E_1^t	E_1^c E_2^c	G
		0.580 0.420	0.032 0.010	0.537
	B	E_b^t	E_b^c	
		0.470	0.180	0.537
		E	E	
	U	0.275	0.275	0.537
	A	0.244	0.244	0.537
Geometric Parameters	Beam length 8.0 in. Beam depth (thickness) 0.6 in. Beam width 1.0 in.			

*M ~ Multimodular, B ~ Bimodular, U ~ Unimodular, A ~ Average Modular.

Table 2. Summary of Cases Considered

Case No.	Boundary Condition and Load Position	Case No.	Boundary Condition and Load Position
1	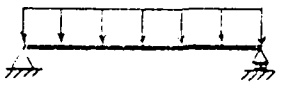	7	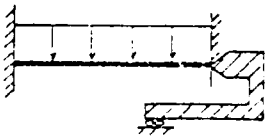
2	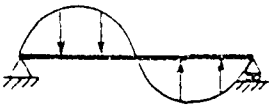	8	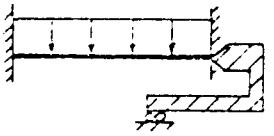
3	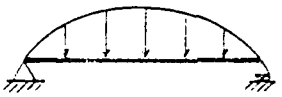	9	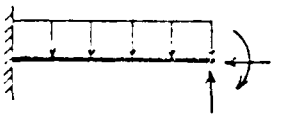
4	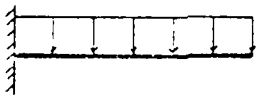	10	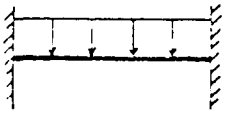
5	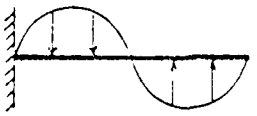	11	
6			

Table 3. Values of K_m and K_q for Various Loadings

Type of Loading	K_m	K_q
Uniform Load $q(x) = q_o$ 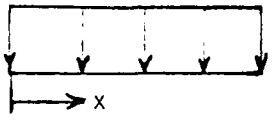	$q_o(\Delta\ell)^2/2$	$q_o\Delta\ell$
Sine Load $q(x) = q_o \sin \frac{n\pi}{\ell} x$ 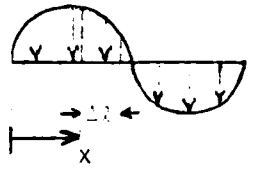	$\frac{q_o\ell}{n\pi}\left[\ell \cos \frac{n\pi}{\ell} x_{j-1} - \frac{\ell}{n\pi}\right.$ $\left.(\sin \frac{n\pi}{\ell} x_j - \sin \frac{n\pi}{\ell} x_{j-1})\right]$	$-\frac{q_o\ell}{n\pi}(\cos \frac{n\pi}{\ell} x_j$ $- \cos \frac{n\pi}{\ell} x_{j-1})$
Cosine Load $q(x) = q_o \cos \frac{n\pi}{\ell} x$ 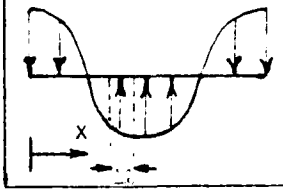	$\frac{q_o\ell}{n}\left[-\frac{\ell}{n\pi}(\cos \frac{n\pi}{\ell} x_j\right.$ $\left.- \cos \frac{n\pi}{\ell} x_{j-1}) - \ell \sin \frac{n\pi}{\ell} x_{j-1}\right]$	$q_o\ell(\sin \frac{n\pi}{\ell} x_j$ $- \sin \frac{n\pi}{\ell} x_{j-1})$

Table 4. Comparison Between Bimodular and Multimodular Cases for Both Closed-Form and Transfer-Matrix Solutions for an Aramid-Rubber Beam (Case 2)‡

x/ℓ	U x 10^4, in.				W x 10^3, in.				ψ x 10^3, rad				M, lb-in.				Q, lb			
	B*		M*		B		M		B		M		B		M		B		M	
	CFS†	TMS†	CFS	TMS	CFS	TMS	CFS	TMS	CFS	TMS	CFS	TMS	CFS	TMS	CFS	TMS	CFS	TMS	CFS	TMS
0.00	0.0000	0.0000	0.0000	0.0000	0.0000	0.0000	0.0000	0.0000	-0.2277	-0.2264	-0.2286	-0.2273	0.0000	0.0000	0.0000	0.0000	0.1273	0.1273	0.1273	0.1273
0.02	-0.0036	-0.0036	-0.0036	-0.0036	0.1121	0.1117	0.1122	0.1118	-0.2259	-0.2246	-0.2268	-0.2255	0.0203	0.0203	0.0203	0.0203	0.1263	0.1263	0.1263	0.1263
0.06	-0.0323	-0.0321	-0.0318	-0.0317	0.3292	0.3272	0.3296	0.3277	-0.2117	-0.2105	-0.2126	-0.2113	0.0597	0.0597	0.0597	0.0597	0.1184	0.1184	0.1184	0.1184
0.10	-0.0878	-0.0873	-0.0865	-0.0861	0.5256	0.5222	0.5263	0.5229	-0.1842	-0.1831	-0.1850	-0.1839	0.0953	0.0953	0.0953	0.0953	0.1030	0.1030	0.1030	0.1030
0.14	-0.1666	-0.1657	-0.1643	-0.1634	0.6890	0.6844	0.6899	0.6853	-0.1451	-0.1443	-0.1457	-0.1449	0.1249	0.1249	0.1249	0.1249	0.0812	0.0812	0.0812	0.0812
0.18	-0.2639	-0.2625	-0.2601	-0.2588	0.8090	0.8036	0.8101	0.8047	-0.0969	-0.0969	-0.0963	-0.0973	0.1467	0.1467	0.1467	0.1467	0.0542	0.0542	0.0542	0.0542
0.22	-0.3734	-0.3714	-0.3681	-0.3662	0.8783	0.8724	0.8795	0.8735	-0.0427	-0.0423	-0.0428	-0.0425	0.1592	0.1592	0.1592	0.1592	0.0239	0.0239	0.0239	0.0239
0.26	-0.4884	-0.4858	-0.4815	-0.4789	0.8924	0.8863	0.8936	0.8875	0.0143	0.0143	0.0144	0.0144	0.1618	0.1618	0.1618	0.1618	-0.0080	-0.0080	-0.0080	-0.0080
0.30	-0.6015	-0.5983	-0.5930	-0.5899	0.8504	0.8446	0.8515	0.8457	0.0704	0.0701	0.0706	0.0704	0.1542	0.1542	0.1542	0.1542	-0.0393	-0.0393	-0.0393	-0.0393
0.34	-0.7057	-0.7020	-0.6957	-0.6921	0.7550	0.7498	0.7560	0.7508	0.1220	0.1215	0.1225	0.1220	0.1369	0.1369	0.1369	0.1369	-0.0682	-0.0682	-0.0682	-0.0682
0.38	-0.7945	-0.7903	-0.7832	-0.7791	0.6121	0.6079	0.6129	0.6087	0.1660	0.1652	0.1667	0.1659	0.1110	0.1110	0.1110	0.1110	-0.0928	-0.0928	-0.0928	-0.0928
0.42	-0.8622	-0.8576	-0.8500	-0.8455	0.4308	0.4278	0.4313	0.4283	0.1995	0.1986	0.2004	0.1994	0.0781	0.0781	0.0781	0.0781	-0.1116	-0.1116	-0.1116	-0.1116
0.46	-0.9046	-0.8998	-0.8918	-0.8871	0.2224	0.2208	0.2227	0.2211	0.2205	0.2195	0.2215	0.2204	0.0403	0.0403	0.0403	0.0403	-0.1233	-0.1233	-0.1233	-0.1233
0.50	-0.9190	-0.9142	-0.9060	-0.9012	0.0000	-0.0000	0.0000	-0.0000	0.2277	0.2266	0.2286	0.2275	0.0000	-0.0000	0.0000	-0.0000	-0.1273	-0.1273	-0.1273	-0.1273
0.54	-0.9046	-0.8998	-0.8918	-0.8871	-0.2224	-0.2209	-0.2227	-0.2211	0.2205	0.2195	0.2215	0.2204	-0.0403	-0.4032	-0.0403	-0.0403	-0.1233	-0.1233	-0.1233	-0.1233
0.58	-0.8622	-0.8576	-0.8500	-0.8455	-0.4308	-0.4278	-0.4313	-0.4284	0.1995	0.1986	0.2004	0.1994	-0.0781	-0.0781	-0.0781	-0.0781	-0.1116	-0.1116	-0.1116	-0.1116
0.62	-0.7945	-0.7903	-0.7832	-0.7791	-0.6121	-0.6079	-0.6129	-0.6087	0.1660	0.1652	0.1667	0.1659	-0.1110	-0.1110	-0.1110	-0.1110	-0.0928	-0.0928	-0.0928	-0.0928
0.66	-0.7057	-0.7020	-0.6957	-0.6921	-0.7545	-0.7498	-0.7560	-0.7508	0.1220	0.1215	0.1225	0.1220	-0.1369	-0.1369	-0.1369	-0.1369	-0.0682	-0.0682	-0.0682	-0.0682
0.70	-0.6015	-0.5983	-0.5930	-0.5899	-0.8504	-0.8446	-0.8515	-0.8457	0.0704	0.0701	0.0706	0.0704	-0.1542	-0.1542	-0.1542	-0.1542	-0.0393	-0.0393	-0.0393	-0.0393
0.74	-0.4884	-0.4858	-0.4815	-0.4789	-0.8924	-0.8863	-0.8936	-0.8875	0.0143	0.0143	0.0144	0.0144	-0.1618	-0.1618	-0.1618	-0.1618	-0.0080	-0.0080	-0.0080	-0.0080
0.78	-0.3734	-0.3714	-0.3681	-0.3662	-0.8783	-0.8724	-0.8795	-0.8735	-0.0427	-0.0423	-0.0428	-0.0425	-0.1592	-0.1592	-0.1592	-0.1592	0.0239	0.0239	0.0239	0.0239
0.82	-0.2639	-0.2625	-0.2601	-0.2587	-0.8090	-0.8036	-0.8101	-0.8047	-0.0969	-0.0963	-0.0973	-0.0967	-0.1467	-0.1467	-0.1467	-0.1467	0.0542	0.0542	0.0542	0.0542
0.86	-0.1666	-0.1657	-0.1643	-0.1634	-0.6890	-0.6844	-0.6899	-0.6853	-0.1451	-0.1443	-0.1457	-0.1449	-0.1249	-0.1249	-0.1249	-0.1249	0.0812	0.0812	0.0812	0.0812
0.90	-0.0878	-0.0873	-0.0865	-0.0860	-0.5256	-0.5222	-0.5263	-0.5229	-0.1842	-0.1831	-0.1850	-0.1839	-0.0953	-0.0953	-0.0953	-0.0953	0.1030	0.1030	0.1030	0.1030
0.94	-0.0323	-0.0321	-0.0318	-0.0316	-0.3292	-0.3272	-0.3296	-0.3277	-0.2117	-0.2105	-0.2126	-0.2114	-0.0597	-0.0597	-0.0597	-0.0597	0.1184	0.1184	0.1184	0.1184
0.98	-0.0036	-0.0036	-0.0036	-0.0036	-0.1121	-0.1117	-0.1122	-0.1119	-0.2259	-0.2246	-0.2268	-0.2255	-0.0203	-0.0203	-0.0203	-0.0203	0.1263	0.1263	0.1263	0.1263
1.00	-0.0000	0.0000	-0.0000	0.0000	0.0000	0.0000	0.0000	0.0000	-0.2277	-0.2264	-0.2286	-0.2273	0.0000	0.0000	-0.0000	-0.0000	0.1273	0.1273	0.1273	0.1273

* B - bimodular and M - multimodular.

† CFS denotes closed-form solution; TMS signifies transfer-matrix solution.

‡ Axial force is zero and z_n is constant for this case [$z_n = \begin{cases} 0.1981 \text{ in. } 0 \le x < \ell/2 \\ 0.1981 \text{ in. } \ell/2 \le x \le \ell \end{cases}$ (for multimodular) and $z_n = \begin{cases} 0.2018 \text{ in. } 0 \le x < \ell/2 \\ -0.2018 \text{ in. } \ell/2 \le x \le \ell \end{cases}$ (for bimodular)]

Table 5. Closed-Form and Transfer-Matrix Solutions for an Aramid-Rubber Beam (Case 3)*

x/ℓ	U x 10^{5}, in.		W x 10^{2}, in.		ψ x 10^{2}, rad		M, lb-in.	Q, lb
	CFS**	TMS**	CFS	TMS	CFS	TMS	CFS & TMS	CFS & TMS
0.00	0.0000	0.0000	0.0000	0.0000	-0.1829	-0.1827	-0.0000	0.2546
0.02	-0.0007	-0.0007	0.0444	0.4443	-0.1825	-0.1823	0.0407	0.2541
0.06	-0.0064	-0.0064	0.1326	0.1323	-0.1797	-0.1794	0.1215	0.2501
0.10	-0.0177	-0.0177	0.2186	0.2182	-0.1704	-0.1737	0.2004	0.2422
0.14	-0.0345	-0.0344	0.3012	0.3006	-0.1655	-0.1653	0.2761	0.2304
0.18	-0.0564	-0.0563	0.3791	0.3783	-0.1544	-0.1542	0.3474	0.2150
0.22	-0.0832	-0.0831	0.4510	0.4500	-0.1409	-0.1407	0.4133	0.1962
0.26	-0.1143	-0.1142	0.5157	0.5146	-0.1252	-0.1250	0.4727	0.1743
0.30	-0.1494	-0.1492	0.5724	0.5711	-0.1075	-0.1074	0.5246	0.1497
0.34	-0.1878	-0.1876	0.6200	0.6186	-0.0881	-0.0880	0.5682	0.1227
0.38	-0.2290	-0.2287	0.6578	0.6564	-0.0673	-0.0672	0.6029	0.0937
0.42	-0.2723	-0.2719	0.6852	0.6837	-0.0455	-0.0454	0.6281	0.0633
0.46	-0.3170	-0.3166	0.7019	0.7004	-0.0229	-0.0229	0.6433	0.0319
0.50	-0.3624	-0.3619	0.7075	0.7059	-0.0000	-0.0000	0.6484	0.0000
0.54	-0.4078	-0.4073	0.7019	0.7004	0.0229	0.0229	0.6433	-0.0319
0.58	-0.4525	-0.4519	0.6852	0.6837	0.0455	0.0454	0.6281	-0.0633
0.62	-0.4958	-0.4952	0.6578	0.6564	0.0673	0.0672	0.6029	-0.0937
0.66	-0.5370	-0.5363	0.6200	0.6186	0.0881	0.0880	0.5682	-0.1227
0.70	-0.5754	-0.5747	0.5724	0.5711	0.1075	0.1074	0.5246	-0.1497
0.74	-0.6105	-0.6097	0.5157	0.5146	0.1252	0.1250	0.4727	-0.1743
0.78	-0.6416	-0.6408	0.4510	0.4500	0.1409	0.1407	0.4133	-0.1962
0.82	-0.6684	-0.6675	0.3791	0.3783	0.1544	0.1542	0.3475	-0.2150
0.86	-0.6903	-0.6894	0.3012	0.3006	0.1655	0.1653	0.2761	-0.2304
0.90	-0.7071	-0.7061	0.2186	0.2182	0.1740	0.1737	0.2004	-0.2422
0.94	-0.7184	-0.7174	0.1326	0.1323	0.1792	0.1794	0.1215	-0.2501
0.98	-0.7241	-0.7231	0.0444	0.0443	0.1825	0.1823	0.0407	-0.2541
1.00	-0.7248	-0.7238	0.0000	0.0000	0.1828	0.1827	-0.0000	-0.2546

*For Case 3, axial force N is zero and z_n is constant, equal to 0.1981 in.
**CFS ∿ closed-form solution; TMS ∿ transfer-matrix solution.

Table 6. Closed-Form and Transfer-Matrix Solutions for an Aramid-Rubber Beam (Case 5)*

x/ℓ	U x 10⁵, in.		W x 10, in.		ψ x 10², rad		M, lb-in.	Q, lb
	CFS**	TMS**	CFS	TMS	CFS	TMS	CFS & TMS	CFS & TMS
0.00	0.0000	0.0000	0.0000	0.0000	0.0000	0.0000	1.0186	0.0000
0.02	-0.0358	-0.0358	-0.0001	-0.0001	0.0180	0.0180	1.0185	-0.0010
0.06	-0.1073	-0.1072	-0.0013	-0.0014	0.0541	0.0542	1.0171	-0.0089
0.10	-0.1786	-0.1785	-0.0038	-0.0039	0.0901	0.0901	1.0120	-0.0243
0.14	-0.2493	-0.2491	-0.0077	-0.0077	0.1258	0.1257	1.0009	-0.0462
0.18	-0.3190	-0.3188	-0.0130	-0.0130	0.1610	0.1609	0.9819	-0.0731
0.22	-0.3870	-0.3867	-0.0198	-0.0198	0.1953	0.1952	0.9537	-0.1035
0.26	-0.4527	-0.4523	-0.0280	-0.0280	0.2285	0.2283	0.9155	-0.1353
0.30	-0.5153	-0.5149	-0.0376	-0.0376	0.2601	0.2599	0.8672	-0.1667
0.34	-0.5743	-0.5738	-0.0485	-0.0486	0.2898	0.2896	0.8091	-0.1955
0.38	-0.6288	-0.6283	-0.0608	-0.0607	0.3174	0.3171	0.7425	-0.2201
0.42	-0.6784	-0.6778	-0.0740	-0.0740	0.3424	0.3421	0.6689	-0.2389
0.46	-0.7226	-0.7220	-0.0883	-0.0882	0.3647	0.3644	0.5903	-0.2506
0.50	-0.7613	-0.7606	-0.1033	-0.1032	0.3842	0.3839	0.5093	-0.2546
0.54	-0.7942	-0.7935	-0.1185	-0.1188	0.4008	0.4005	0.4282	-0.2506
0.58	-0.8215	-0.8208	-0.1349	-0.1347	0.4146	0.4143	0.3497	-0.2389
0.62	-0.8434	-0.8428	-0.1511	-0.1509	0.4257	0.4254	0.2761	-0.2201
0.66	-0.8604	-0.8599	-0.1674	-0.1671	0.4343	0.4340	0.2094	-0.1955
0.70	-0.8730	-0.8725	-0.1835	-0.1833	0.4406	0.4404	0.1514	-0.1666
0.74	-0.8819	-0.8815	-0.1995	-0.1993	0.4451	0.4449	0.1030	-0.1353
0.78	-0.8877	-0.8874	-0.2152	-0.2150	0.4480	0.1479	0.0648	-0.1035
0.82	-0.8912	-0.8909	-0.2306	-0.2304	0.4498	0.4497	0.0366	-0.0731
0.86	-0.8931	-0.8928	-0.2458	-0.2455	0.4508	0.4506	0.0177	-0.0462
0.90	-0.8939	-0.8937	-0.2606	-0.2603	0.4512	0.4510	0.0066	-0.0243
0.94	-0.8942	-0.8940	-0.2752	-0.2750	0.4513	0.4512	0.0014	-0.0089
0.98	-0.8942	-0.8940	-0.2897	-0.2895	0.4513	0.4512	0.0005	-0.0010
1.00	-0.8942	-0.8940	-0.2970	-0.2967	0.4513	0.4512	0.0000	0.0000

*For Case 5, axial force N is zero and z_n is constant, equal to 0.1981 in.
**CFS ≈ closed-form solution; TMS ≈ transfer-matrix solution.

Table 7. Closed-Form and Transfer-Matrix Solutions for an Aramid-Cord Rubber Beam (Case 6)*

x/ℓ	U x 10⁴, in.		W x 10, in.		ψ x 10², rad		M, lb-in.	Q, lb
	CFS**	TMS**	CFS	TMS	CFS	TMS	CFS & TMS	CFS & TMS
0.00	0.0000	0.0000	0.0000	0.0000	-0.0000	0.0000	-2.0372	0.5093
0.02	0.0070	0.0070	0.0033	0.0033	-0.0354	-0.0354	-1.9557	0.5088
0.06	0.0202	0.0202	0.0116	0.0116	-0.1018	-0.1018	-1.7934	0.5048
0.10	0.0322	0.0322	0.0218	0.0218	-0.1625	-0.1626	-1.6331	0.4968
0.14	0.0431	0.0431	0.0338	0.0337	-0.2176	-0.2177	-1.4759	0.4851
0.18	0.0529	0.0529	0.0472	0.0471	-0.2672	-0.2673	-1.3230	0.4696
0.22	0.0617	0.0617	0.0620	0.0619	-0.3115	-0.3115	-1.1757	0.4509
0.26	0.0695	0.0695	0.0778	0.0777	-0.3506	-0.3507	-1.0348	0.4290
0.30	0.0763	0.0763	0.0946	0.0944	-0.3849	-0.3850	-0.9014	0.4043
0.34	0.0822	0.0822	0.1121	0.1119	-0.4146	-0.4148	-0.7763	0.3773
0.38	0.0872	0.0872	0.1301	0.1299	-0.4401	-0.4402	-0.6601	0.3484
0.42	0.0914	0.0915	0.1485	0.1484	-0.4616	-0.4617	-0.5535	0.3180
0.46	0.0950	0.0950	0.1672	0.1670	-0.4794	-0.4796	-0.4567	0.2866
0.50	0.0979	0.0979	0.1860	0.1858	-0.4941	-0.4943	-0.3701	0.2546
0.54	0.1002	0.1003	0.2048	0.2047	-0.5058	-0.5061	-0.2938	0.2227
0.58	0.1020	0.1021	0.2236	0.2235	-0.5150	-0.5153	-0.2275	0.1913
0.62	0.1034	0.1035	0.2423	0.2422	-0.5220	-0.5224	-0.1712	0.1609
0.66	0.1045	0.1045	0.2609	0.2607	-0.5273	-0.5276	-0.1244	0.1320
0.70	0.1052	0.1053	0.2792	0.2791	-0.5310	-0.5313	-0.0865	0.1050
0.74	0.1057	0.1058	0.2974	0.2972	-0.5335	-0.5339	-0.0569	0.0803
0.78	0.1060	0.1061	0.3153	0.3152	-0.5351	-0.5355	-0.0348	0.0584
0.82	0.1062	0.1063	0.3330	0.3329	-0.5360	-0.5365	-0.0192	0.0396
0.86	0.1063	0.1064	0.3505	0.3505	-0.5365	-0.5370	-0.0091	0.0242
0.90	0.1063	0.1064	0.3679	0.3679	-0.5367	-0.5372	-0.0033	0.0124
0.94	0.1064	0.1064	0.3852	0.3852	-0.5368	-0.5373	-0.0007	0.0045
0.98	0.1064	0.1065	0.4024	0.4024	-0.5368	-0.5373	-0.0000	0.0005
1.00	0.1064	0.1065	0.4110	0.4110	-0.5368	-0.5373	-0.0000	0.0000

*For Case 6, axial force N is zero and z_n is constant, equal to -0.1981 in.
**CFS ∿ closed-form solutions, TMS ∿ transfer-matrix solutions.

Table 8. Closed-Form and Transfer-Matrix Solutions for an Aramid-Cord Rubber Beam (Case 7)*

x/ℓ	U x 10^{4}, in.		W x 10^{2}, in.		ψ x 10^{1}, rad		M, lb-in.		Q, lb
	CFS**	TMS**	CFS	TMS	CFS	TMS	CFS	TMS	CFS & TMS
0.00	0.0000	0.0000	0.0000	0.0000	0.0000	0.0000	-0.5333	-0.5325	0.4000
0.02	0.1762	0.1760	0.0241	0.0241	-0.0889	-0.0888	-0.4706	-0.4698	0.3840
0.06	0.4648	0.4645	0.0733	0.0731	-0.2346	-0.2345	-0.3528	-0.3520	0.3520
0.10	0.6742	0.6740	0.1227	0.1224	-0.3403	-0.3402	-0.2453	-0.2445	0.3200
0.14	0.8118	0.8116	0.1710	0.1707	-0.4097	-0.4096	-0.1480	-0.1472	0.2880
0.18	0.8846	0.8844	0.2172	0.2168	-0.4464	-0.4464	-0.0610	-0.0602	0.2560
0.22	0.8999	0.8997	0.2603	0.2598	-0.4542	-0.4541	0.0158	0.0160	0.2240
0.26	0.8648	0.8647	0.2995	0.2989	-0.4365	-0.4364	0.0823	0.0822	0.1920
0.30	0.7866	0.7865	0.3338	0.3332	-0.3970	-0.3969	0.1387	0.1395	0.1600
0.34	0.6724	0.6723	0.3628	0.3621	-0.3394	-0.3393	0.1848	0.1856	0.1280
0.38	0.5295	0.5294	0.3859	0.3852	-0.2672	-0.2672	0.2206	0.2214	0.0960
0.42	0.3650	0.3649	0.4027	0.4020	-0.1842	-0.1842	0.2615	0.2470	0.0640
0.46	0.1861	0.1861	0.4129	0.4121	-0.9392	-0.9391	0.2616	0.2624	0.0320
0.50	-0.0000	-0.0000	0.4163	0.4156	-0.0000	-0.0000	0.2667	0.2675	-0.0000
0.54	-0.1861	-0.1861	0.4129	0.4121	0.9392	0.9390	0.2616	0.2624	-0.0320
0.58	-0.3650	-0.3649	0.4027	0.4020	0.1842	0.1842	0.2615	0.2624	-0.0640
0.62	-0.5295	-0.5294	0.3859	0.3852	0.2672	0.2672	0.2206	0.2214	-0.0960
0.66	-0.6724	-0.6723	0.3628	0.3621	0.3394	0.3393	0.1848	0.1856	-0.1280
0.70	-0.7866	-0.7865	0.3338	0.3332	0.3970	0.3969	0.1387	0.1395	-0.1600
0.74	-0.8648	-0.8647	0.2995	0.2989	0.4365	0.4364	0.0823	0.0822	-0.1920
0.78	-0.8999	-0.8997	0.2603	0.2598	0.4542	0.4541	0.0158	0.0160	-0.2240
0.82	-0.8846	-0.8844	0.2172	0.2168	0.4464	0.4464	-0.0610	-0.0602	-0.2560
0.86	-0.8118	-0.8116	0.1710	0.1707	0.4097	0.4069	-0.1480	-0.1472	-0.2880
0.90	-0.6742	-0.6740	0.1227	0.1224	0.3403	0.3402	-0.2453	-0.2445	-0.3200
0.94	-0.4648	-0.4645	0.0733	0.0731	0.2346	0.2345	-0.3528	-0.3520	-0.3520
0.98	-0.1762	-0.1760	0.0241	0.0241	0.0889	0.0888	-0.4706	-0.4698	-0.3840
1.00	0.0000	0.0000	0.0000	0.0000	0.0000	0.0000	-0.5333	-0.5325	-0.4000

*For Case 7, axial force N is zero and z_η constant, equal to 0.1981 in.
**CFS ∿ closed-form solutions; TMS ∿ transfer-matrix solutions.

Table 9. Closed-Form and Transfer-Matrix Solutions for an Aramid-Cord Rubber Beam (Case 8)*

x/ℓ	U x 10^4, in.		W x 10^3, in.		ψ x 10^3, rad		M, lb-in.		Q, lb	
	CFS**	TMS**	CFS	TMS	CFS	TMS	CFS	TMS	CFS	TMS
0.00	0.0000	0.0000	0.0000	0.0000	0.0000	0.0000	-0.0949	-0.0945	0.1510	0.1509
0.02	0.0291	0.0289	0.0911	0.0908	-0.0147	-0.0146	-0.0708	-0.0704	0.1500	0.1499
0.06	0.0622	0.0619	0.2739	0.2723	-0.0314	-0.0312	-0.0238	-0.0235	0.1421	0.1420
0.10	0.0635	0.0632	0.4455	0.4426	-0.0320	-0.0320	0.0193	0.0197	0.1267	0.1266
0.14	0.0364	0.0363	0.5926	0.5886	-0.0184	-0.0183	0.0566	0.0569	0.1049	0.1048
0.18	-0.0141	-0.0139	0.7042	0.6993	0.0071	0.0070	0.0859	0.0862	0.0779	0.0778
0.22	-0.0821	-0.0816	0.7717	0.7663	0.0414	0.0412	0.1061	0.1063	0.0476	0.0475
0.26	-0.1608	-0.1598	0.7906	0.7844	0.0812	0.0806	0.1162	0.1164	0.0157	0.0156
0.30	-0.2430	-0.2416	0.7573	0.7519	0.1227	0.1219	0.1162	0.1164	-0.0156	-0.0157
0.34	-0.3218	-0.3199	0.6754	0.6706	0.1624	0.1614	0.1065	0.1066	-0.0445	-0.0446
0.38	-0.3906	-0.3883	0.5495	0.5456	0.1971	0.1960	0.0882	0.0883	-0.0691	-0.0692
0.42	-0.4440	-0.4415	0.3876	0.3849	0.2241	0.2228	0.0629	0.0629	-0.0878	-0.0880
0.46	-0.4778	-0.4751	0.2004	0.1989	0.2412	0.2398	0.0327	0.0327	-0.0996	-0.0997
0.50	-0.4894	-0.4866	0.0000	-0.0000	0.2413	0.2456	-0.0000	-0.0000	-0.1036	-0.1037
0.54	-0.4778	-0.4751	-0.2004	-0.1989	0.2412	0.2398	-0.0327	-0.0327	-0.0996	-0.0997
0.58	-0.4440	-0.4415	-0.3876	-0.3849	0.2241	0.2228	-0.0629	-0.0629	-0.0878	-0.0880
0.62	-0.3906	-0.3883	-0.5495	-0.5456	0.1971	0.1960	-0.0882	-0.0883	-0.0691	-0.0692
0.66	-0.3218	-0.3199	-0.6754	-0.6706	0.1624	0.1614	-0.1065	-0.1066	-0.0445	-0.0446
0.70	-0.2430	-0.2416	-0.7573	-0.7519	0.1227	0.1219	-0.1162	-0.1164	-0.0156	-0.0157
0.74	-0.1608	-0.1598	-0.7906	-0.7844	0.0812	0.0806	-0.1162	-0.1164	0.0157	0.0156
0.78	-0.0821	-0.0816	-0.7717	-0.7663	0.0414	0.0412	-0.1061	-0.1063	0.0476	0.0475
0.82	-0.0141	-0.0139	-0.7042	-0.6993	0.0071	0.0070	-0.0859	-0.0862	0.0779	0.0778
0.86	0.0364	0.0363	-0.5926	-0.5886	-0.0184	-0.0183	-0.0566	-0.0569	0.1049	0.1048
0.90	0.0635	0.0632	-0.4455	-0.4426	-0.0320	-0.0320	-0.0193	-0.0197	0.1267	0.1266
0.94	0.0622	0.0619	-0.2739	-0.2723	-0.0314	-0.0312	0.0238	0.0235	0.1421	0.1420
0.98	0.0291	0.0289	-0.0911	-0.0908	-0.0147	-0.0146	-0.0708	0.0704	1.1500	0.1499
1.00	0.0000	0.0000	-0.0000	-0.0000	0.0000	0.0000	0.0949	0.0945	0.1510	0.1509

*For Case 8, axial force N is zero and z_n is constant, $z_n = \begin{cases} 0.1981 \text{ in.} & 0.0 \leq x/\ell < 0.5 \\ -0.1981 \text{ in.} & 0.5 \leq x/\ell \leq 1.0 \end{cases}$

**CFS ∿ closed-form solutions; TMS ∿ transfer-matrix solutions.

Table 10. Transfer-Matrix Solutions for an Aramid-Cord Rubber Beam (Case 11)*

x/ℓ	U x 10^{4}, in.	W x 10^{2}, in.	ψ x 10^{3}, rad	M, lb-in.	Q, lb
0.00	0.0000	0.0000	0.0000	-0.4123	0.2546
0.02	0.1376	0.0157	-0.0695	-0.3716	0.2541
0.06	0.3702	0.0499	-0.1868	-0.2908	0.2501
0.10	0.5467	0.0867	-0.2759	-0.2119	0.2422
0.14	0.6689	0.1247	-0.3376	-0.1362	0.2304
0.18	0.7395	0.1626	-0.3732	-0.0648	0.2150
0.22	0.7619	0.1992	-0.3845	0.0011	0.1962
0.26	0.7403	0.2335	-0.3737	0.0642	0.1743
0.30	0.6797	0.2642	-0.3430	0.1123	0.1497
0.34	0.5854	0.2907	-0.2955	0.1560	0.1227
0.38	0.4637	0.3121	-0.2341	0.1906	0.0937
0.42	0.3210	0.3278	-0.1620	0.2158	0.0633
0.46	0.1641	0.3374	-0.0828	0.2311	0.0319
0.50	-0.0000	0.3406	-0.0000	0.2362	-0.0000
0.54	-0.1641	0.3374	0.0828	0.2311	-0.0319
0.58	-0.3210	0.3278	0.1620	0.2158	-0.0633
0.62	-0.4637	0.3121	0.2341	0.1906	-0.0937
0.66	-0.5854	0.2907	0.2955	0.1560	-0.1227
0.70	-0.6797	0.2642	0.3430	0.1123	-0.1497
0.74	-0.7403	0.2335	0.3737	0.0642	-0.1743
0.78	-0.7619	0.1992	0.3845	0.0011	-0.1962
0.82	-0.7395	0.1626	0.3732	-0.0648	-0.2150
0.86	-0.6689	0.1247	0.3376	-0.1362	-0.2304
0.90	-0.5467	0.0867	0.2759	-0.2119	-0.2422
0.94	-0.3702	0.0499	0.1868	-0.2908	-0.2501
0.98	-0.1376	0.0157	0.0695	-0.3716	-0.2541
1.00	0.0000	0.0000	0.0000	-0.4123	-0.2546

*For Case 11, axial force due to bending-stretching coupling (N) is -0.3070×10^{-4} lb (compressive), also $z_n = 0.1918$ in.

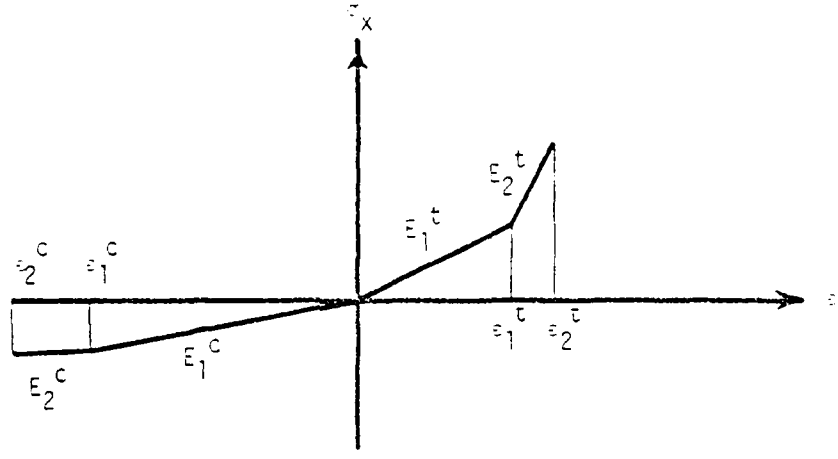

Fig. 1 Multimodular model.

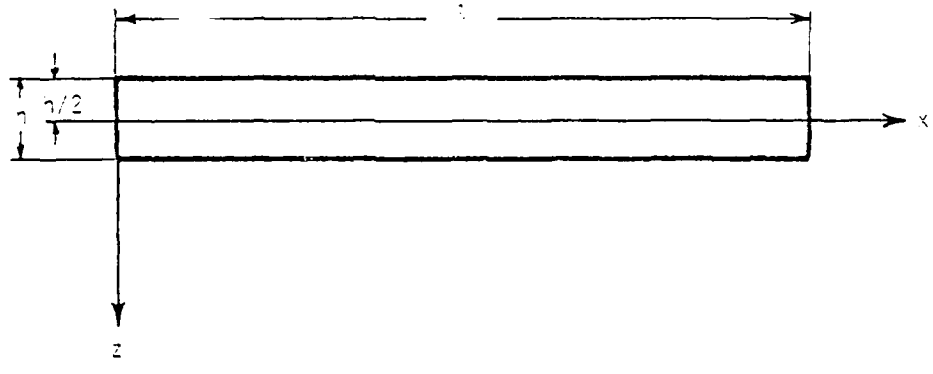

Fig. 2 Geometry of beam.

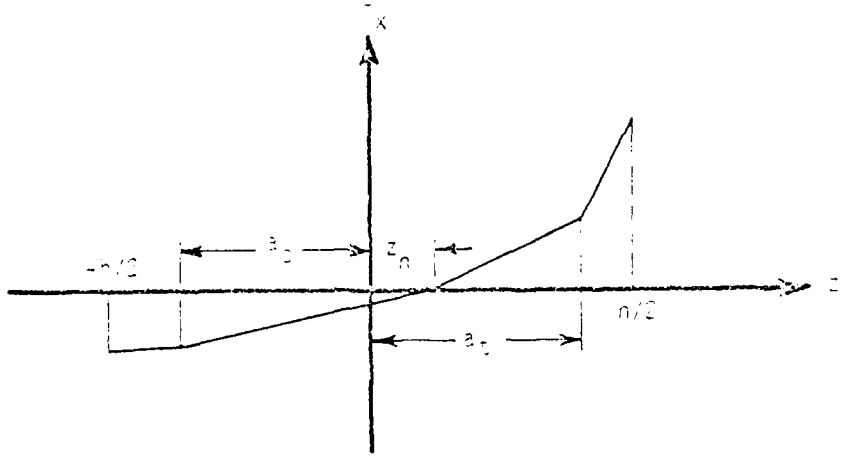

Fig. 3 Stress distribution for convex bending case.

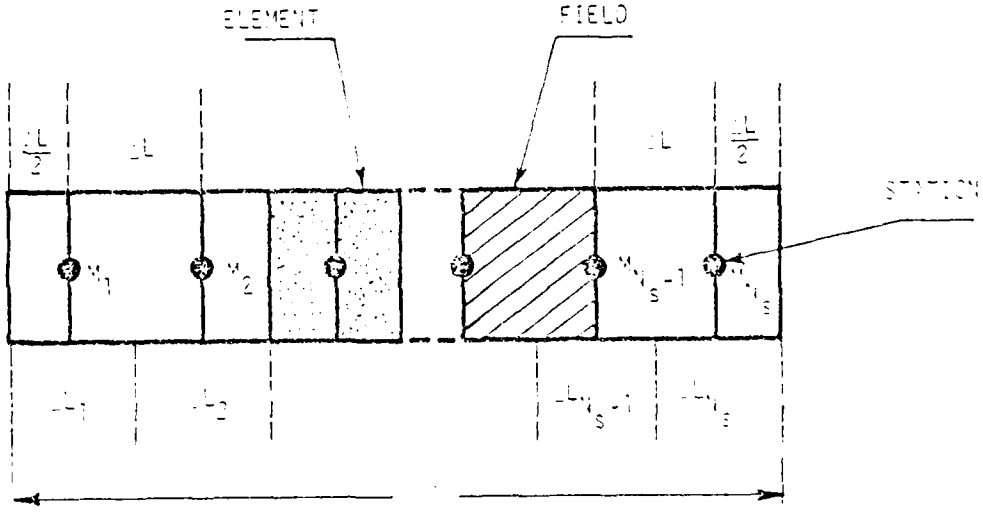

Fig. 4 Mesh for transfer-matrix analysis.

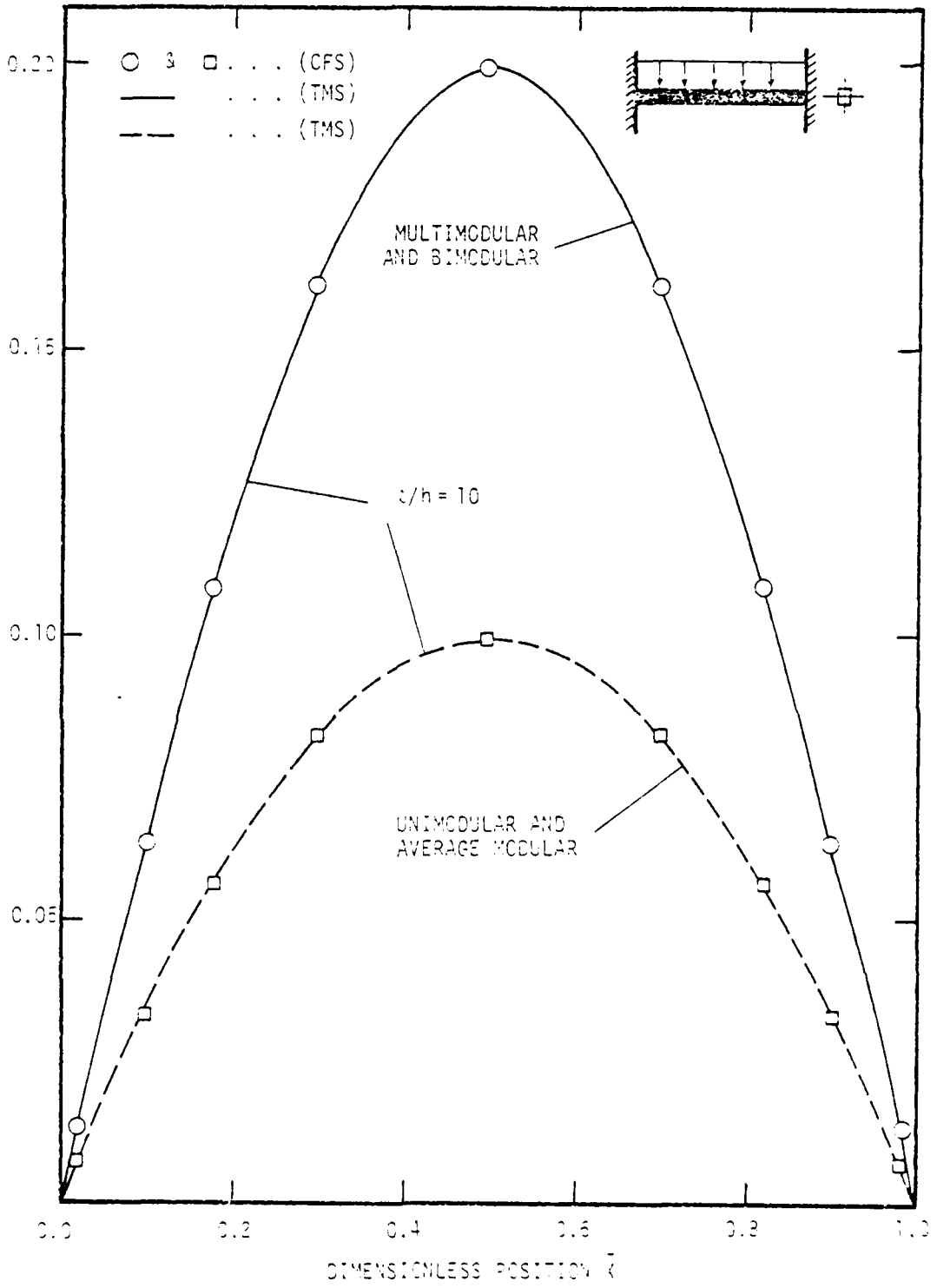

Fig. 8 Comparison among multimodular, bimodular, unimodular, and average modular deflection distributions for closed-form and transfer-matrix solutions of clamped-clamped aramid-cord rubber beam ($\bar{s}/h = 10$).

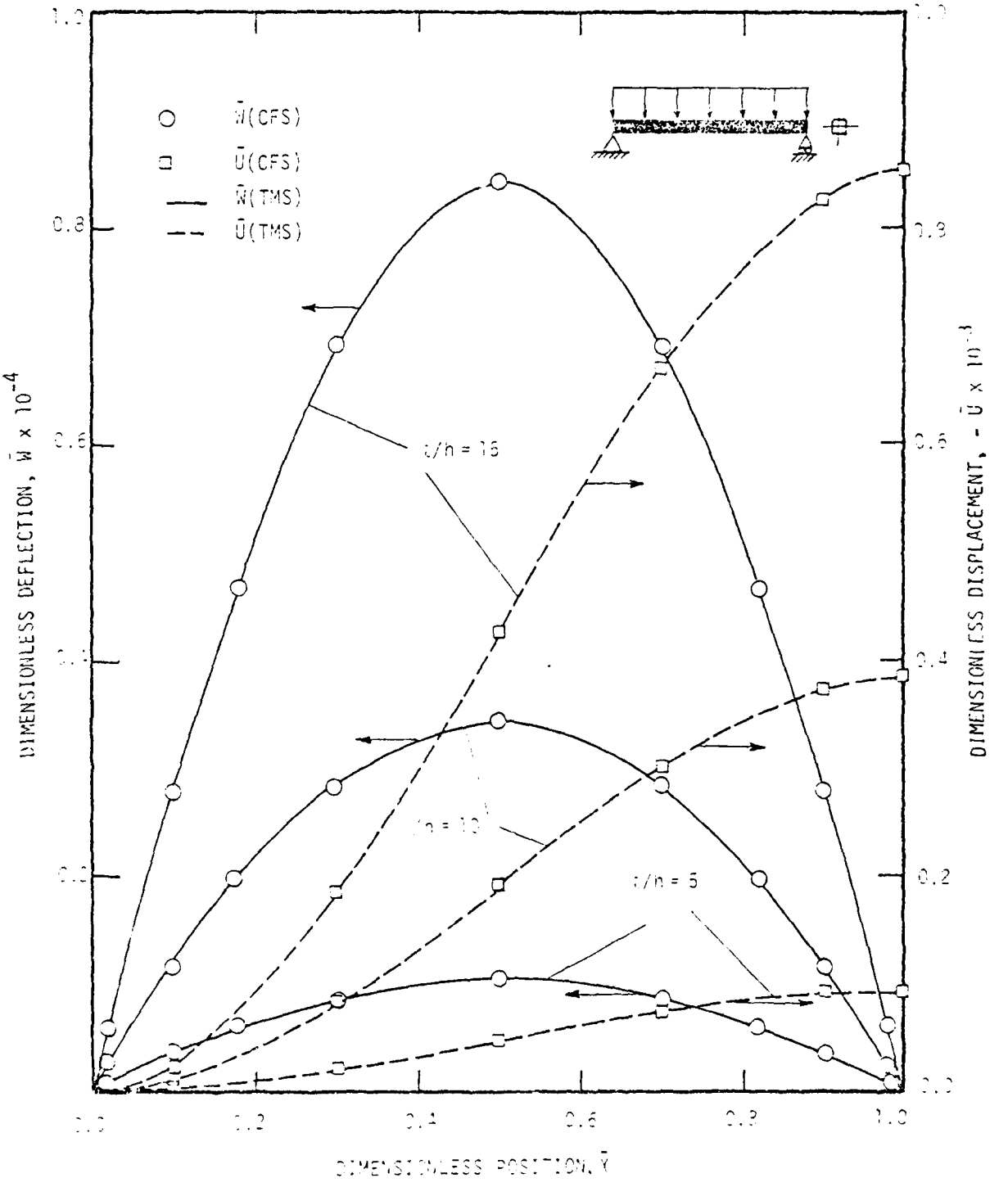

Fig. 6 Closed-form and transfer-matrix solutions of pinned-pinned, sandwich-type rubber beam with rectangular cross section (L/h = 5, 10, 15).

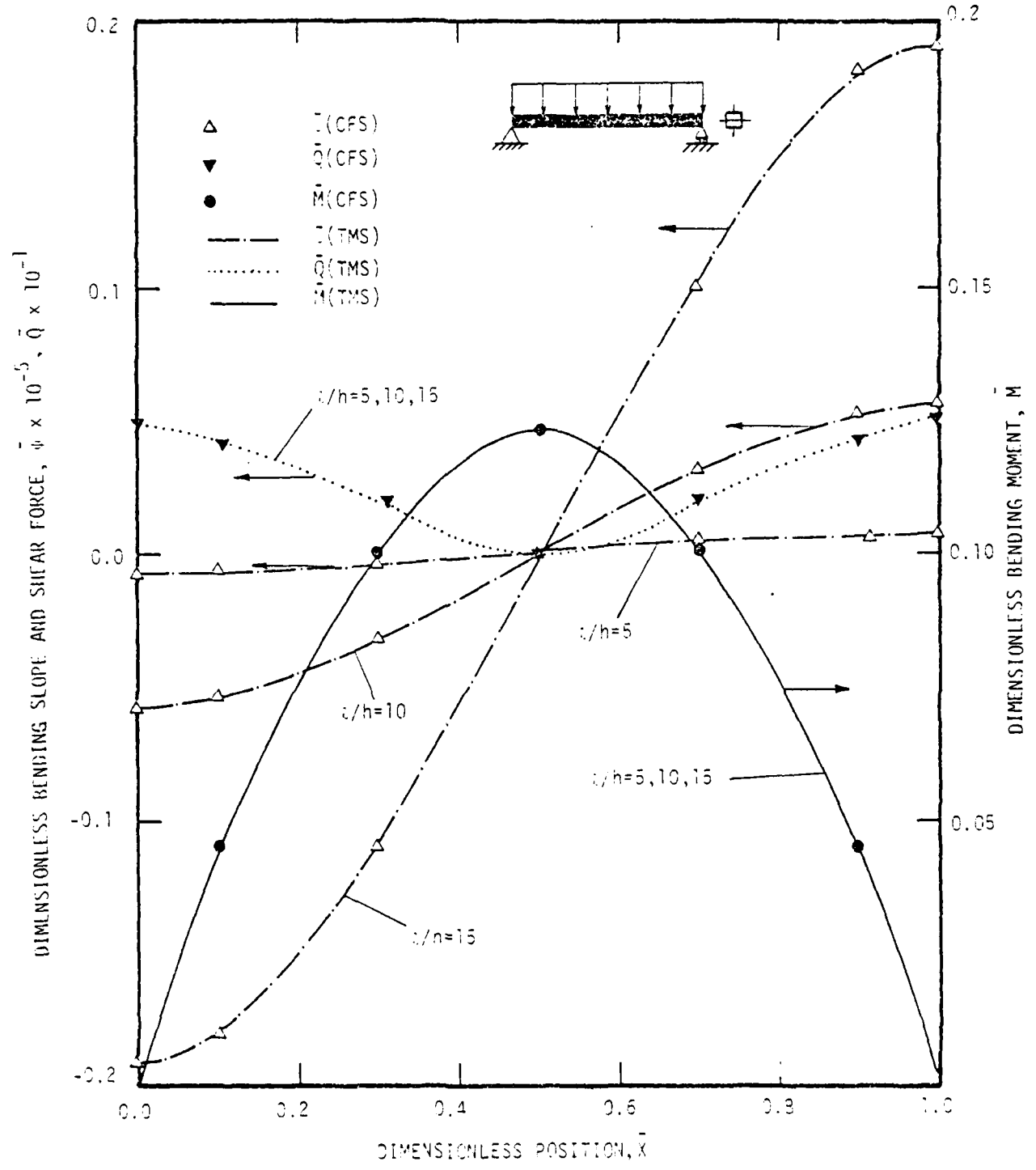

Fig. 7 Closed-form and transfer-matrix solutions of hinged-hinged, aramid-cord rubber beam with rectangular cross section (ℓ/h = 5, 10, 15).

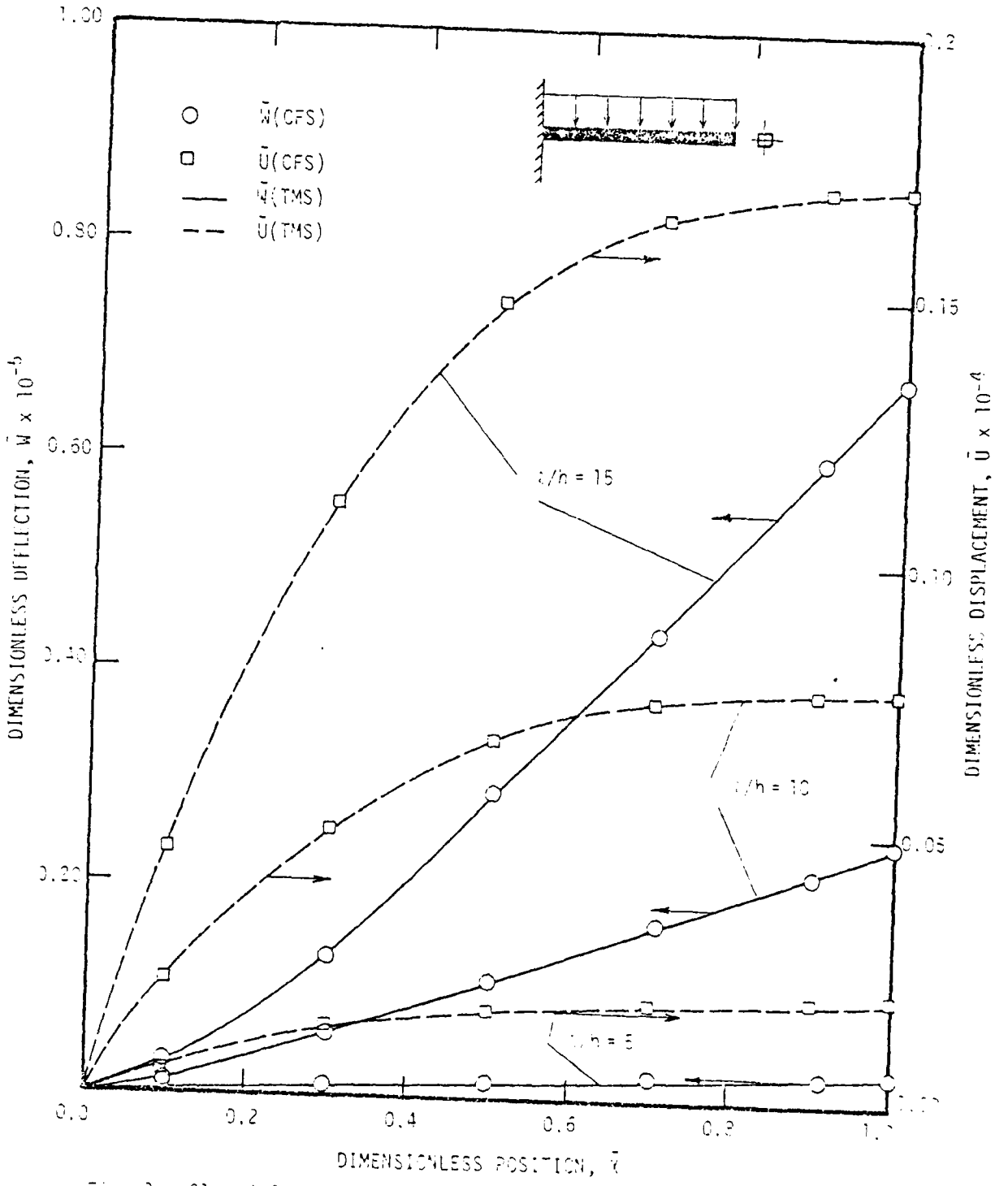

Fig. 8 Closed-form and transfer-matrix solutions of clamped-free, aramid-cord rubber beam with rectangular cross section (L/h = 5, 10, 15).

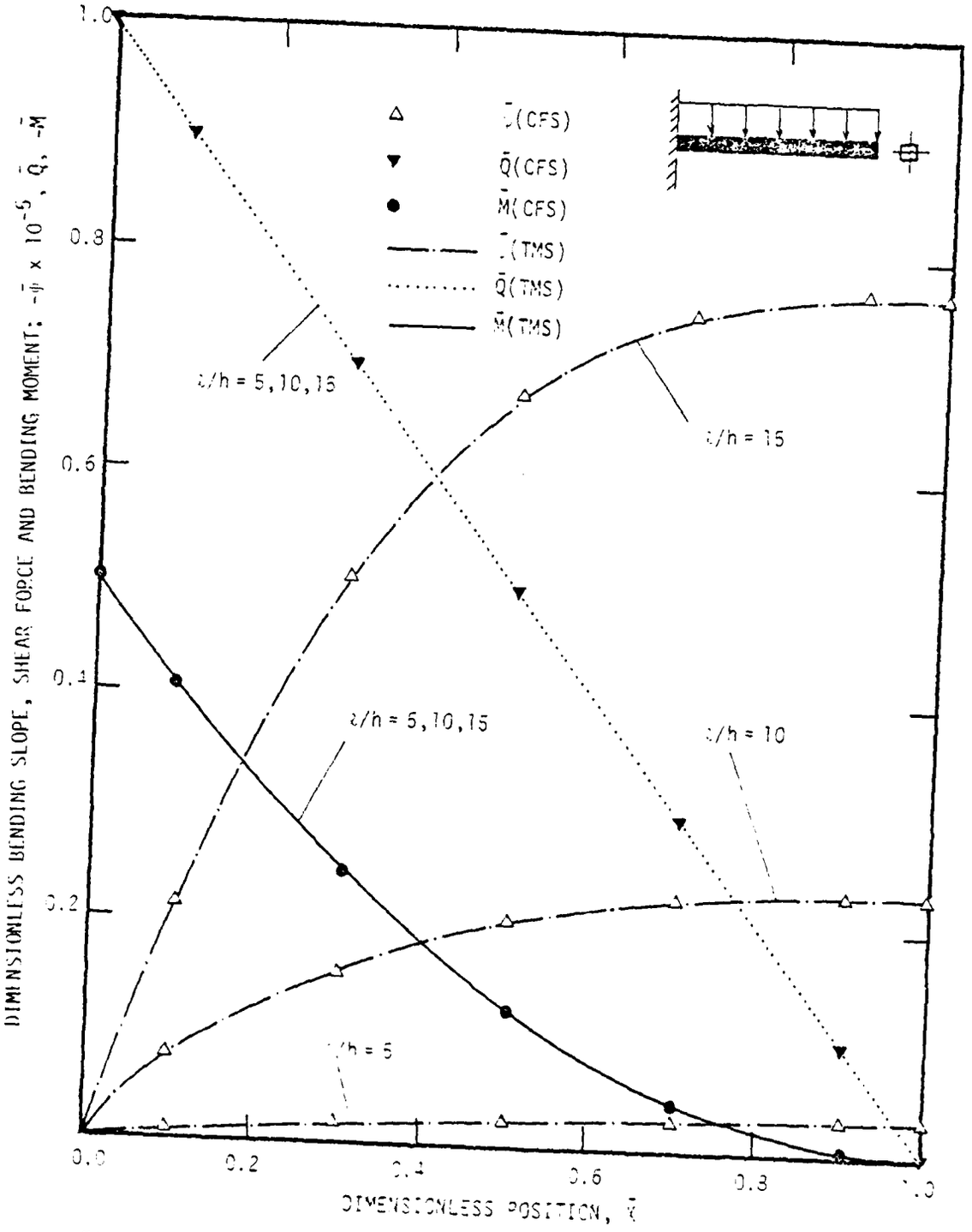

Fig. 9 Closed-form and transfer-matrix solutions of clamped-free, aramid-cord rubber beam with rectangular cross section (ℓ/h = 5, 10, 15).

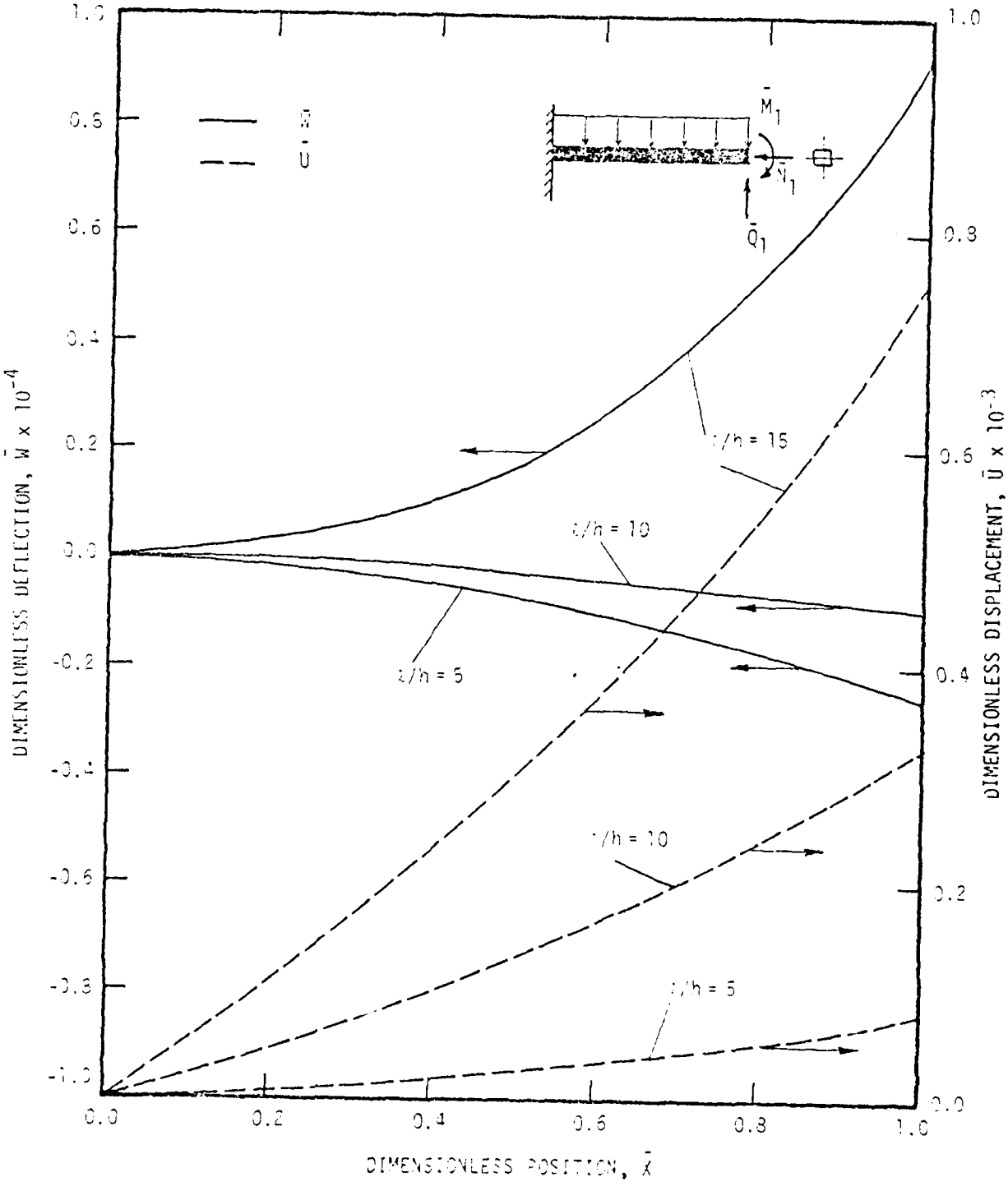

Fig. 10 Transfer-matrix solution of clamped-free, aramid-cord rubber beam with rectangular cross section and applied force and moment at the free end (ℓ/h = 5, 10, 15).

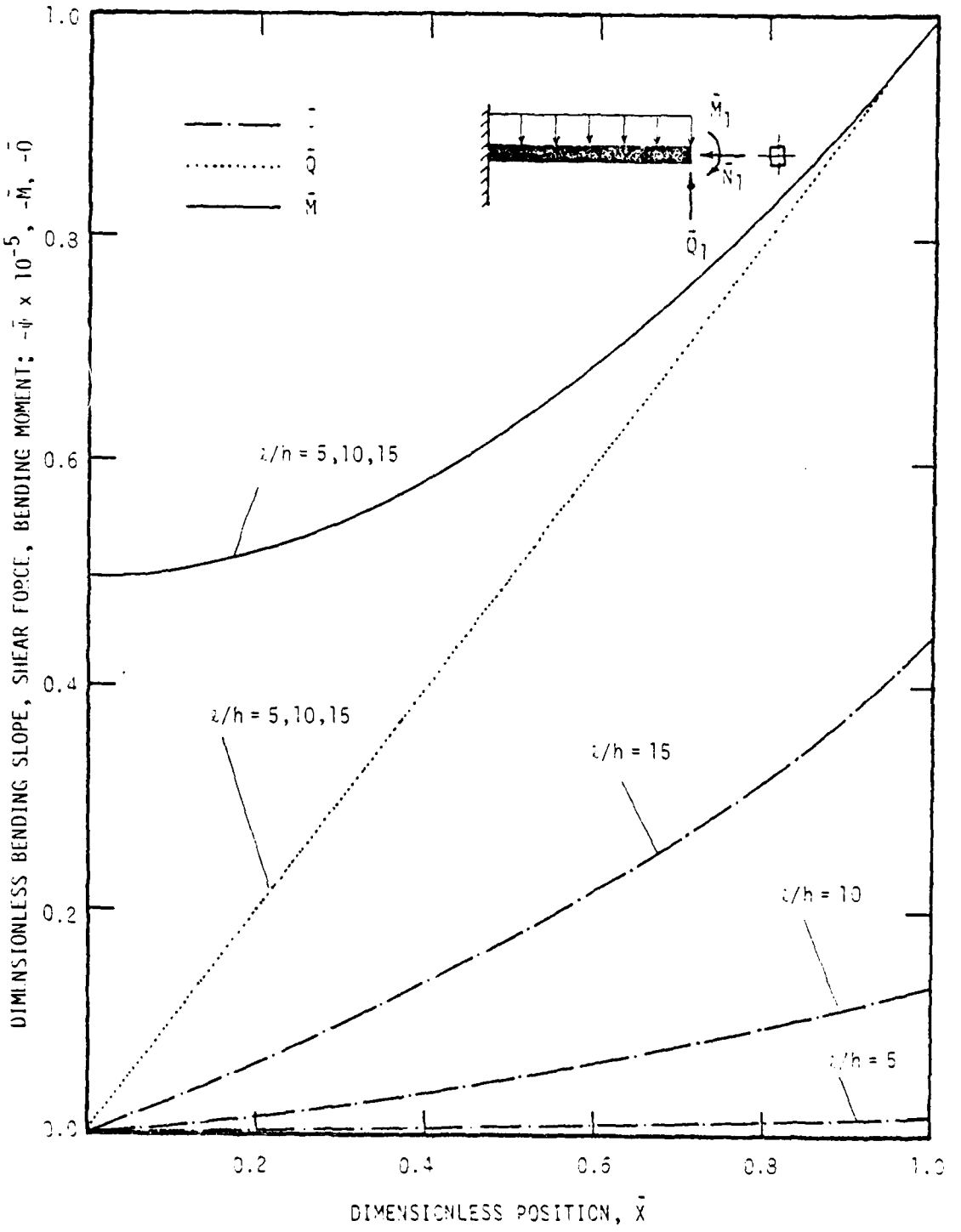

Fig. 11 Transfer-matrix solution of clamped-free, aramid-cord rubber beam with rectangular cross section and applied force and moment at the free end (ℓ/h = 5, 10, 15).

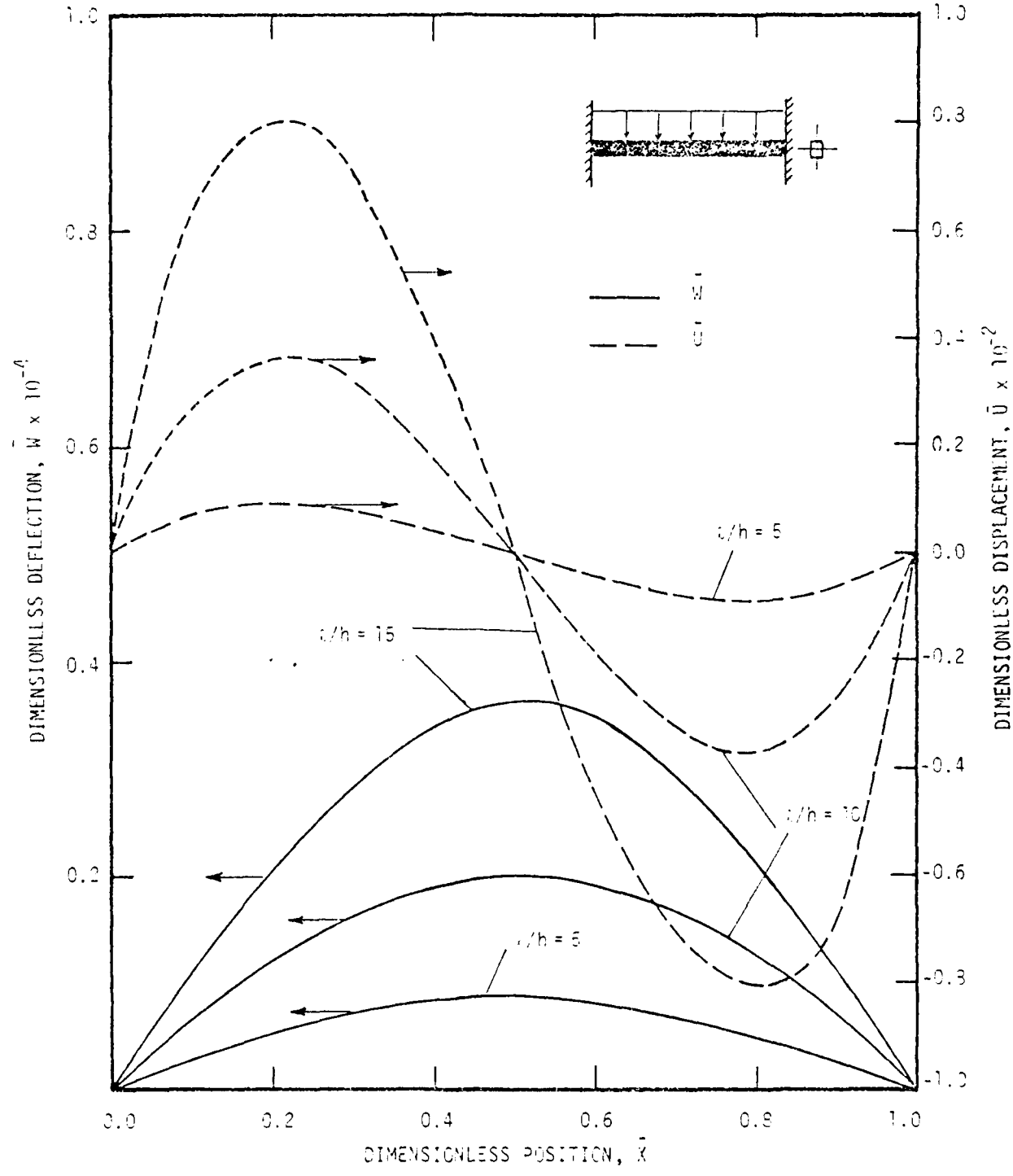

Fig. 12 Transfer-matrix solution of clamped-clamped, aramid-cord rubber beam with rectangular cross section (L/h = 5, 10, 15).

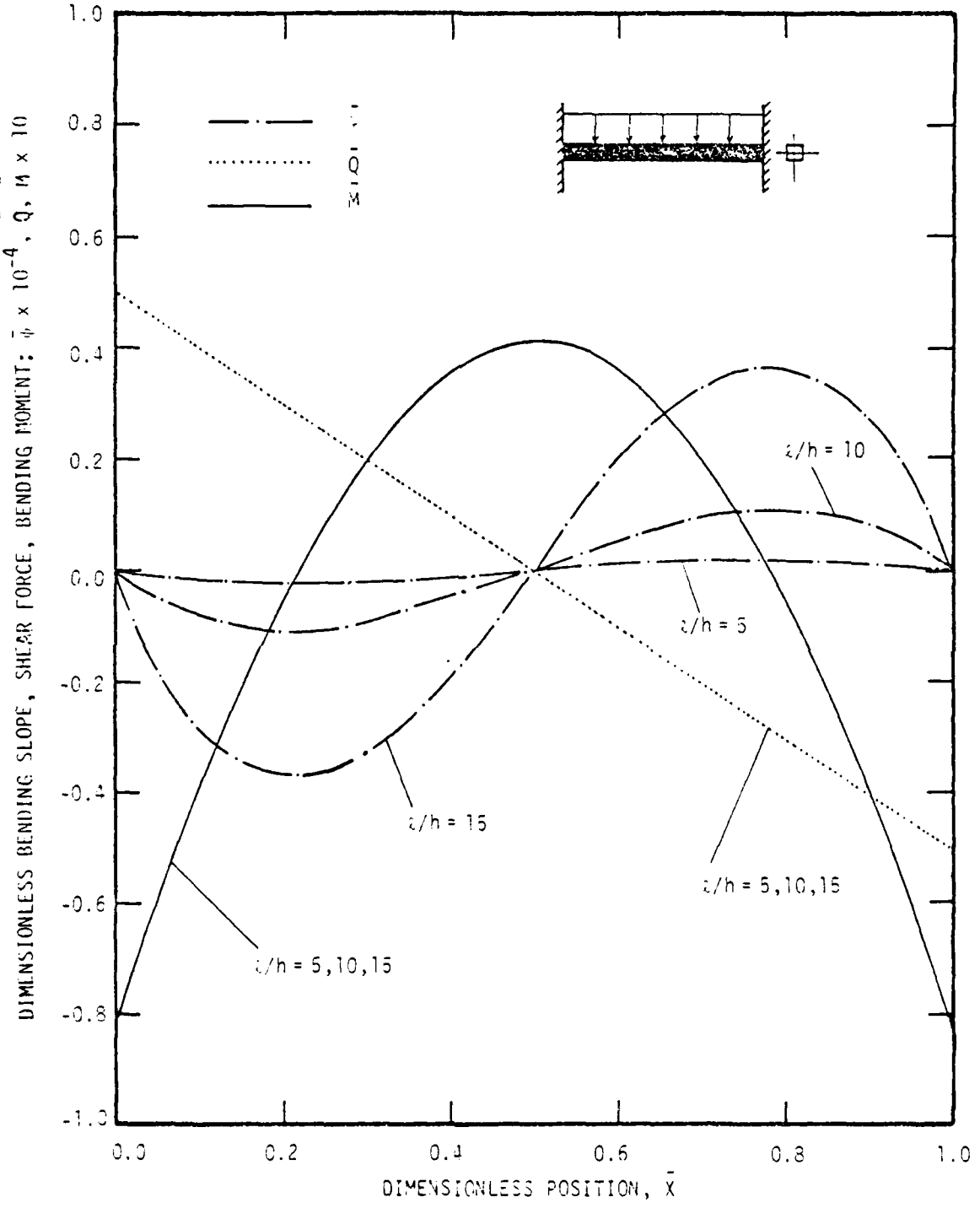

Fig. 13 Transfer-matrix solution of clamped-clamped, aramid-cord rubber beam with rectangular cross section (ℓ/h = 5, 10, 15).

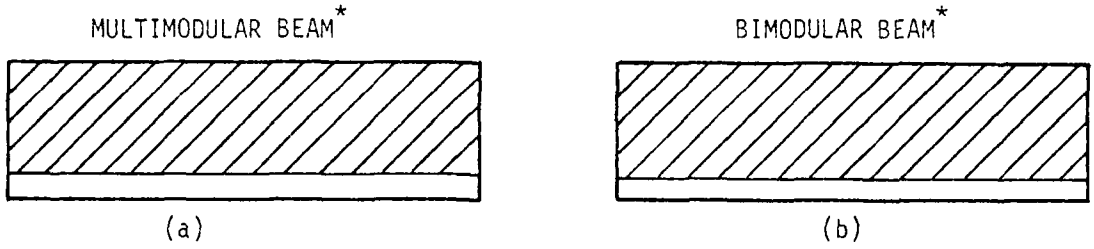

Fig. 14 Cases 1, 3, 7, 10, and 11

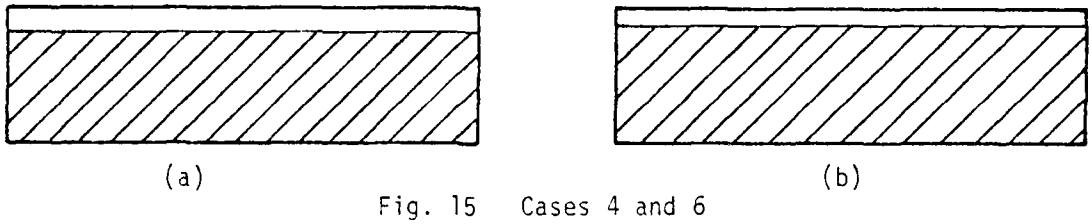

Fig. 15 Cases 4 and 6

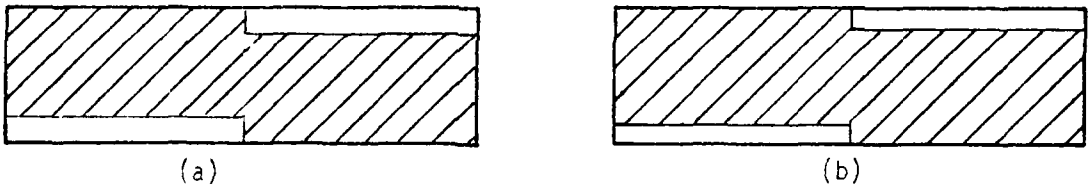

Fig. 16 Cases 2, 5, and 8

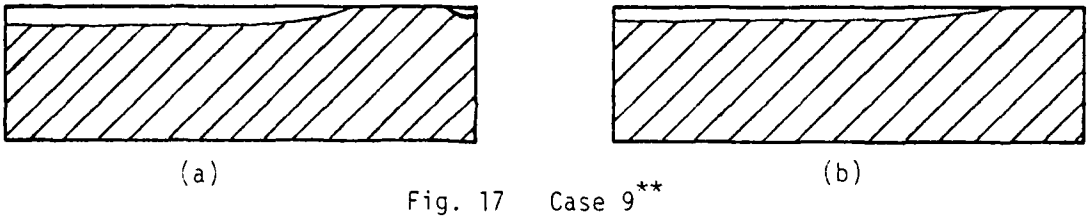

Fig. 17 Case 9**

*Computations are applicable to a specific beam (see Table 1).
**For Case 9: $M_1 = -0.1$ lb-in., $N_1 = -1.0$ lb, and $Q_1 = -0.1$ lb.

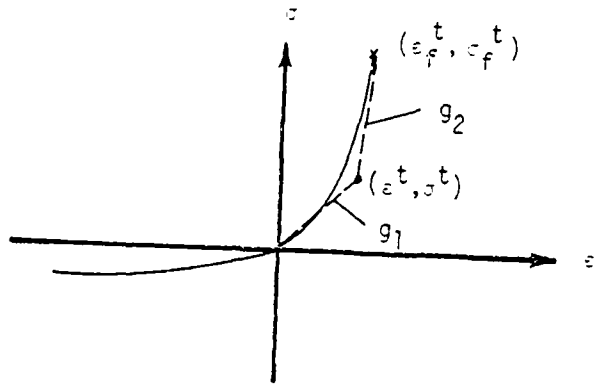

Fig. A.1 Multimodular model.

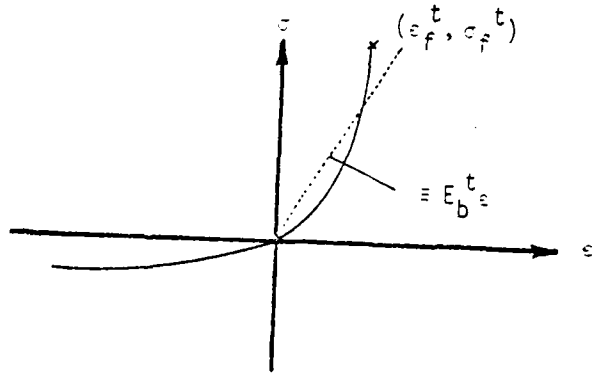

Fig. A.2 Bimodular model.

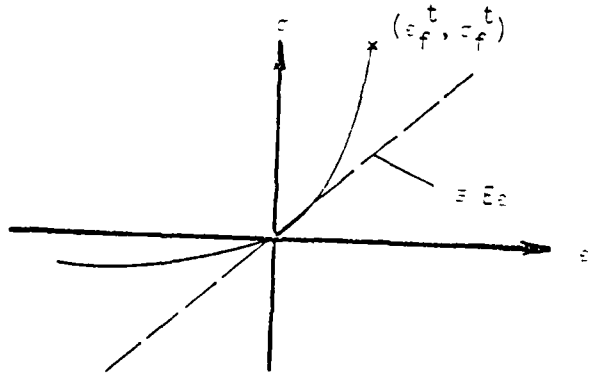

Fig. A.3 Unimodular model.

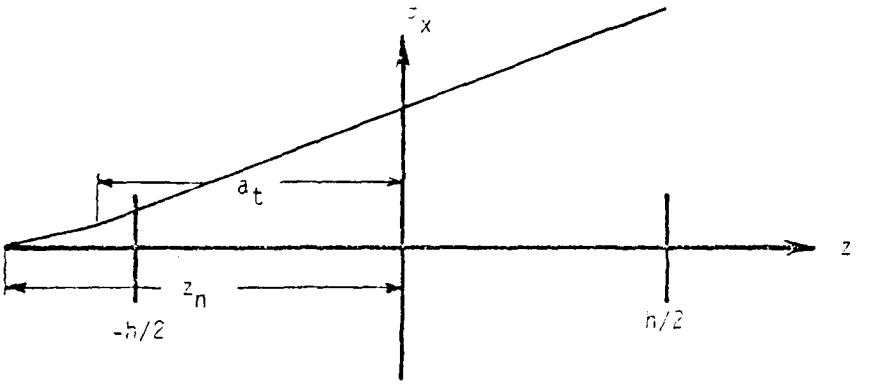

Fig. 8.1 Stress distribution for Case 1.

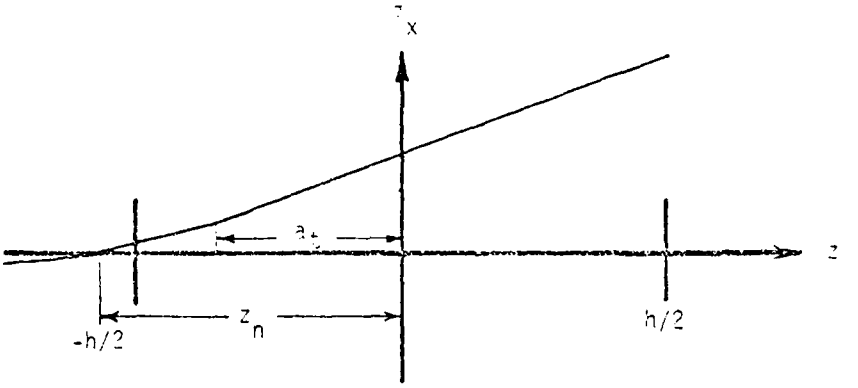

Fig. 8.2 Stress distribution for Case 2.

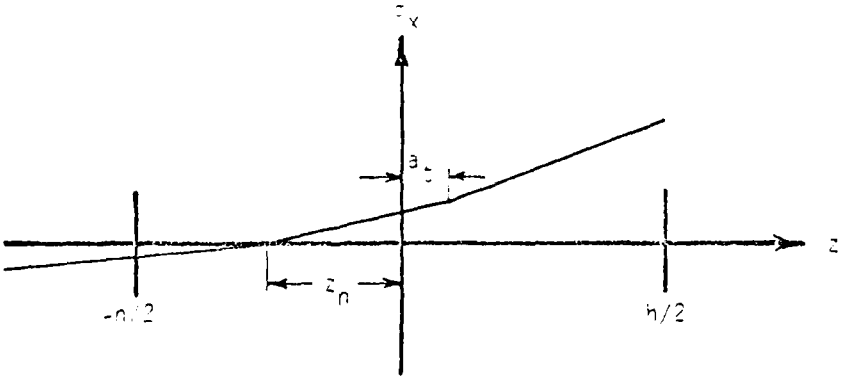

Fig. 8.3 Stress distribution for Case 3.

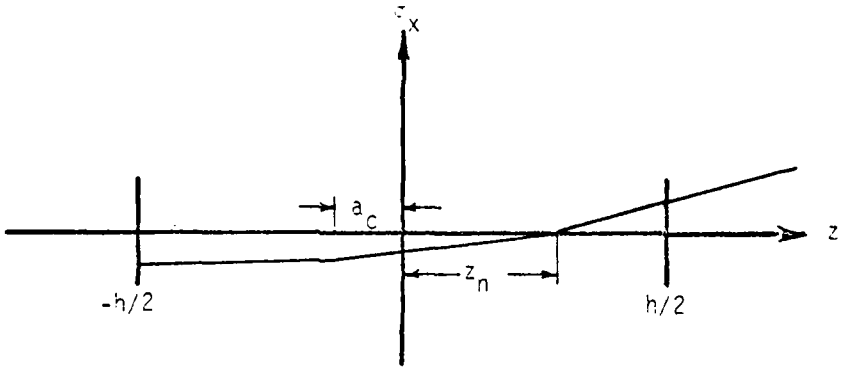

Fig. B.4 Stress distribution for Case 5.

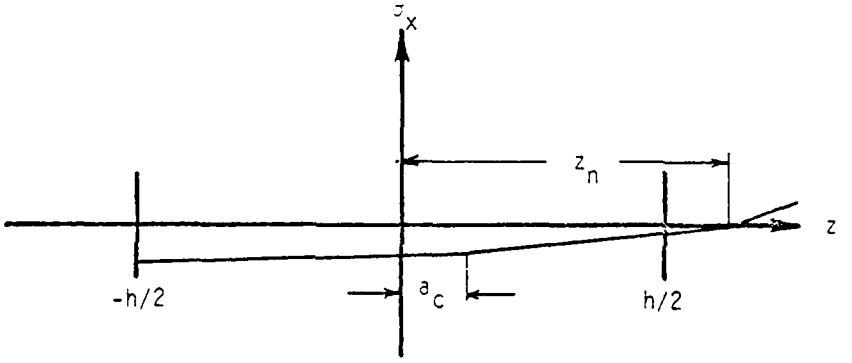

Fig. B.5 Stress distribution for Case 6.

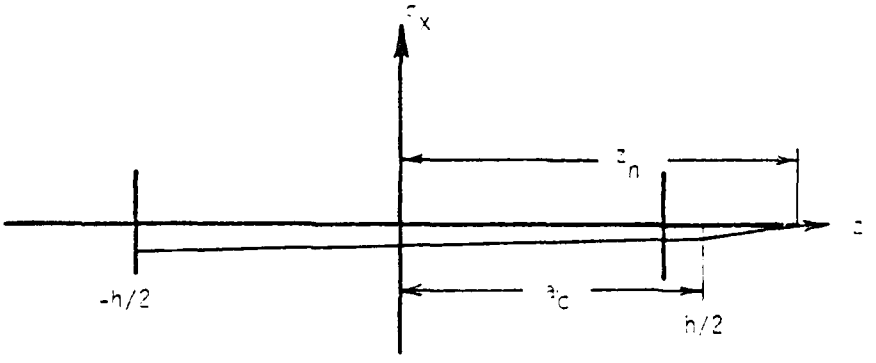

Fig. B.6 Stress distribution for Case 7.

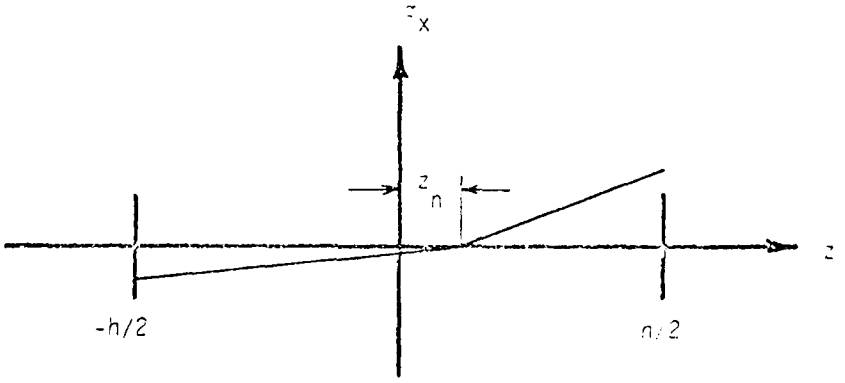

Fig. B.7 Stress distribution for Case B.

PART II

PREDICTION OF BENDING RUPTURE STRENGTH OF NON-LINEAR MATERIALS WITH DIFFERENT BEHAVIOR IN TENSION AND COMPRESSION

Charles W. Bert
The University of Oklahoma
Norman, Oklahoma 73019

Abstract - Many materials have quite different stress-strain relations in tension and compression. Examples include such diverse materials as rock, cast iron, concrete, tire cord-rubber, and soft biological tissues. It is shown by analysis in this paper that DBTC (different behavior in tension and compression) has a profound effect on the flexural strength as predicted by application of fundamental continuum mechanics relations. The theory is applied to a non-linear material model which is shown to be applicable to two widely different materials: concrete, which has more strength degradation in tension than in compression, and steel cord-rubber, which has strength which is enhanced in tension by cord strengthening and degraded in compression by cord microbuckling.

1. INTRODUCTION

It has long been known that certain materials behave significantly differently in tension than in compression. For example, this was recognized by Saint-Venant [1], who analyzed the pure bending behavior of a beam having different non-linear stress-strain curves in tension and compression. Specific experimental evidence of DBTC has been reported for cast iron by Gilbert [2], cord-rubber by Clark [3], polymers by Zemlyakov [4], concrete by Seefried et al. [5], cortical bone by Simkin and Robin [6], various kinds of rock by Haimson and Tharp [7], and soft biological tissue by Pearsall and Roberts [8]. Of course, the specific micromechanisms reponsible for DBTC vary from one class of material to another. Stiff, brittle solids are weakened in tension by microcracks, while soft fiber-reinforced materials are weakened in compression by fiber microbuckling.

In this paper, a general theory is presented for the prediction of the maximum bending moment achievable in unidirectional pure bending for an arbitrary material with DBTC. Subsequently, the general theory is applied to a simple model which is suitable for widely different materials: concrete using a continuous damage mechanics model for the tensile behavior, and cord-rubber.

2. GENERAL THEORY

The theory developed here is an extension of the basic theory of unidirectional bending developed by Bach and Baumann [9]; see Nadai [10], section 22-1. The material is assumed to be subjected to a unidirectional pure bending moment, i.e., there is no applied direct tension or compression. The beam cross section and loading are assumed to be symmetric about the same axis, so that bending takes place in a single plane (no twisting or warping).

Poisson-type lateral contraction effects are neglected* and the beam cross section is assumed to be sufficiently compact that cross-sectional distortion (ovalization and warping) and buckling do not occur. Plane sections are assumed to remain plane so that the axial strain ε is given

$$\varepsilon = \kappa z \tag{1}$$

where z is the normal position coordinate, measured positive downward from the neutral-surface position, and κ is the bending curvature.

The beam material may have arbitrary uniaxial stress-strain behavior in the longitudinal direction, i.e.,

$$\sigma = \begin{cases} \sigma_t(\varepsilon) & \varepsilon > 0 \\ \sigma_c(\varepsilon) & \varepsilon < 0 \end{cases} \tag{2}$$

where σ is the axial normal stress and $\sigma_t(\varepsilon)$ and $\sigma_c(\varepsilon)$ are arbitrary continuous functions.

In the absence of direct axial loading, equilibrium of forces in the axial direction requires

$$\int_{-C_c}^{0} \sigma_c(\kappa z)b(z)dz + \int_{0}^{C_t} \sigma_t(\kappa z)b(z)dz = 0 \tag{3}$$

Here the respective compressive and tensile outer-fiber distances are denoted by C_c and C_t and the cross-sectional width at distance z is denoted by $b(z)$; see Fig. 1. Substituting specific expressions for $b(z)$, $\sigma_c(\kappa z)$, and $\sigma_t(\kappa z)$ into (1), integrating, and using the following geometric relation (see Fig. 1) allows determination of C_c and C_t:

$$C_c + C_t = H \tag{4}$$

Equilibrium of the internal moment due to the stress distribution with the externally applied bending moment M gives

---

*This assumption is more reasonable for bending than for tension loading, and more reasonable for brittle materials, such as concrete and rock, than for ductile metals such as considered by Bert et al. [11].

$$\int_{-C_c}^{0} z\sigma_c(\kappa z)b(z)dz + \int_{0}^{C_t} z\sigma_t(\kappa z)b(z)dz = M \qquad (5)$$

The ultimate bending moment is found by using differential calculus to determine the relative maximum, i.e.

$$M = M_{max} \text{ when } dM/dp = 0 \qquad (6)$$

where p is any convenient parameter which can be used as a measure of deformation.

In principle, the general theory can be applied to any material (provided that it has continuous but different* stress-strain curves in tension and compression) with any singly-symmetric cross section. The similarity with the theory of ductile failure by plastic tensile instability originated by Considere [12] is readily apparent; c.f., Nadai [10], section 8-1.

3. A NON-LINEAR MATERIAL MODEL

The following mathematical relationship is proposed to approximate the stress-strain behavior of a variety of actual materials:

$$\sigma = \begin{cases} \sigma_c(\varepsilon) = E_c\varepsilon + F_c\varepsilon^2 & ; \quad \varepsilon < 0 \\ \sigma_t(\varepsilon) = E_t\varepsilon + F_t\varepsilon^2 & ; \quad \varepsilon > 0 \end{cases} \qquad (7)$$

where E_c and E_t are the Young's moduli in compression and tension and F_c and F_t are also material constants. This model can be considered to be a generalization of Krajcinovic's model for plain concrete [14]. In this case,

$$E_c = E_t = E, \quad F_c = 0, \quad F_t = -E^2/D_t \qquad (8)$$

where D_t is a tensile-microcrack-damage modulus ($D_t>0$) related to Janson and Hult's linear version [15] of Kachanov's concept of continuum damage mechanics

---

*The case of damage induced instability in beam bending for materials having the same continuous damage in tension and compression was considered by Boström [13].

[16]. For an excellent review of CDM, the reader is referred to Hult [17].

The present model is an improvement on the Krajcinovic model in that it also includes compressive non-linearity as suggested by British Standard CP110 [18]:

$$F_c = -E^2/4f_{cu} \tag{9}$$

where f_{cu} is the material's ultimate strength in uniaxial compression (see Appendix A2).

To apply equation (7) to unidirectional cord-rubber, using experimental data for cord rubber reported by Bert and Kumar [19], one has $E_t \approx E_c$, $F_c = F_t > 0$.

If one assumes a rectangular beam of width B, application of equation (7) in equation (3) yields:

$$\frac{1}{2} B\kappa(E_tC_t^2-E_cC_c^2) + \frac{1}{3} B\kappa^2(F_tC_t^3+F_cC_c^3) = 0$$

or

$$\kappa = \frac{3}{2} \frac{E_cC_c^2-E_tC_t^2}{F_tC_t^3+F_cC_c^3} \tag{10}$$

Integrating equation (5), using equation (7), one obtains

$$M = \frac{1}{3} B\kappa(E_tC_t^3+E_cC_c^3) + \frac{1}{4} B\kappa^2(F_tC_t^4-F_cC_c^4) \tag{11}$$

Substituting the expression for κ from equation (10) into equation (11) and using equation (4) to eliminate C_c, one finally obtains the following expression for M as a function of C_t:

$$M = (B/2) \frac{[E_c(H-C_t)^2-E_tC_t^2][E_tC_t^3+E_c(H-C_t)^3]}{F_tC_t^3 + F_c(H-C_t)^3}$$

$$+ (9B/16)\frac{[F_tC_t^4 - F_c(H-C_t)^4][E_c(H-C_t)^2-E_tC_t^2]^2}{[F_tC_t^3 + F_c(H-C_t)^3]^2} \tag{12}$$

Of course, the ultimate bending moment (M_u) can be found as a function of B,H,E_c,E_t,F_c, and F_t by either direct substitution or use of differential calculus ($dM/dC_t = 0$).

4. APPLICATION TO PLAIN CONCRETE

Bert and Kumar [20] showed that for Krajcinovic's [14] material [$E_c = E_t = E$, $F_c = 0$, and F_t given by equation (8)], equation (12) takes a form that can be expressed as

$$M = 6[1-(15/8)K_t + (3/4)K_t^2][K_t^{-2}-(1/2)K_t^{-3}] \tag{13}$$

where $M \equiv 6M/BD_tH^2$ and $K_t \equiv C_t/H$. Bert and Kumar showed that the ultimate value of m, m_u, is 0.407 at $K_t = 0.5875$. These values are both slightly higher than the values $m_u = 0.354$ at $K_t = 0.5505$ obtained by Krajcinovic, who used the following failure criterion, which is appropriate only for failure in uniform uniaxial tension

$$d\sigma/d\varepsilon = 0 \tag{14}$$

It is traditional to report ultimate strength data in bending in terms of bending rupture strength defined as the maximum tensile stress at ultimate bending moment calculated according to the simple, purely elastic formula

$$f_{bu} = M_uC/I \tag{15}$$

where

$$I = BH^3/12 \quad ; \quad C = H/2 \tag{16}$$

It is to be emphasized that the value obtained by use of equation (15) is <u>not</u> a stress value; it is just an index of moment-carrying ability expressed in units of force per unit area.

Combining the definition of m_u ($\equiv 6M_u/D_tBH^2$) with equations (15) and (16), one can easily show that

$$f_{bu} = D_tm_u \tag{17}$$

It is shown in Appendix A1 that use of the criterion $d\sigma/d\varepsilon$ for uniform axial loading leads to the following expression for the ultimate tensile strength:

$$f_{tu} = D_t/4 \tag{18}$$

Thus,

$$f_{bu}/f_{tu} = 4m_u \qquad (19)$$

Fig. 2 shows a comparison among the experimental data of Gonnerman and Shuman [21] and of Brooks and Neville [22] (both wet and dry stored) and the theoretical prediction of Krajcinovic [14] and of Bert and Kumar [20].

It is noted that the Krajcinovic and Bert and Kumar predictions both are f_{bu} vs. f_{tu} relations that are straight lines starting at the origin (with slopes of 1.42 and 1.63, respectively). However, the experimental curves are straight lines shifted upward so that they have f_{bu} intercepts. Apparently this upward shift is due to statistical considerations, such as considered by Weil and Daniel [23], for instance, using the Weibull distribution [24] and by Jayatilaka [25], using a different approach.

It is well known that concrete has a stress-strain non-linearity in compression, although less pronounced than the one in tension. This was recognized in British Standard CP110 [18]; see also Refs. [26-30]. This non-linearity is represented by the term in equation (7) with a coefficient F_c. To obtain a quantitative value for F_c, one must know either

(1) the mean compressive stress-strain curve to failure

(2) the mean compressive strength (f_{cu}), for it is shown in Appendix A2 that $F_c = E^2/Dc$ where $D_c = 4f_{cu}$.

(3) the ratio of mean compressive strength to mean tensile strength for $D_c/D_t = f_{cu}/f_{tu}$.

Since the author has not yet been able to obtain a copy of Ref. [21], it is necessary to consider typical values of f_{cu}/f_{tu}. (Ref. [22] had $f_{cu}/f_{tu} \approx 15$.) From statistical considerations, for various values of the Weibull parameter and sample size, Jayatilaka [25], Table 5.13, gave values of f_{cu}/f_{tu} ranging from 3 to 20. However, the ratio f_{bu}/f_{tu} predicted by the present theory is not strongly affected by f_{cu}/f_{tu}, as can be seen in Table 1.

Piechnik and Pachla [31] proposed a power-law damage function to describe the tensile behavior of plain concrete. An analysis using this damage function to predict failure in bending and in tension is presented in Appendix B. For n = 4, the value recommended by Piechnik and Pachla, $\sigma_{bu}/D = m_u = 0.715$ at a value of 0.529 for K_t for the bending case. For tension, a value of 0.669 is attained for σ_{tu}/D. Thus,

$$\sigma_{bu}/\sigma_{tu} = 0.715/0.669 = 1.07$$

This value of 1.07 is considerably lower than is consistent with the experimental results of Refs. [21] and [22]. The explanation for this discrepancy may be any one of the following factors or a combination of them:

(1) Difference in details of cement, composition and fineness, aggregrate size, material quality, and curing [32] between the 1928 American concrete [21] and the 1977 British concrete [22] on one hand and the 1979 Polish concrete [31] on the other.

(2) Increase in measured σ_{bu}/σ_{tu} due to a brittle failure mechanism and statistical size effects as discussed previously.

(3) Possibility that the material damage relation for concrete has a threshold effect, as suggested by Young [33] and Bert and Kumar [20], rather than the Piechnik power-law damage function suggested in [31].

5. APPLICATION TO CORD-REINFORCED RUBBER

It was shown in the recent experiments of Bert and Kumar [19] that the stress-strain relations of this class of materials is strongly dependent upon the type of cord. For example, aramid-rubber loaded in the cord direction (0°) has a drastic discontinuity in slope at the origin ($E_c > E_t$), yet the same material loaded at 90° to the cord direction is very nearly linearly through ($E_c = E_t$, $F_c = F_t = 0$). As an example of the application of the

generalized model presented in Section 3, steel cord-rubber specially made to have highly waved cords is considered. Then $E_c \approx E_t = E$ and $F_c = F_t = F > 0$. Then equation (12) simplifies to

$$M/BH^2 = (E^2/F)(1-2K_t)\left[3 - \frac{27}{8}(1-2K_t+2K_t^2)\left(\frac{1-2K_t}{3K_t^2-3K_t+1}\right)^2\right] \qquad (20)$$

It can be shown that the maximum vlaue of dimensionless bending moment is $6M_uF/BE^2H^2 = 0.433$ at a value of 0.380 for K_t. Now due to the monotonically increasing slope of the tension portion of the stress-strain curve, it does not exhibit a maximum-load phenomenon. (Tensile failure is obviously due to another mechanism, probably cord failure.) Thus, in this case, it is necessary to ratio the bending strength to the compressive strength rather than the tensile strength. From Appendix A2, one has

$$\sigma_{cu} = -E^2/4F \qquad (21)$$

Thus,

$$|\sigma_{tu}/\sigma_{cu}| = \frac{6M_u/BH^2}{E^2/4F} = 1.73$$

This indicates that σ_{bu} is 1.73 times the compressive strength. In reality, the tension portion of the steel-cord rubber is even steeper than indicated by a power of two. Thus, σ_{bu} would be expected to be even greater. This could not be verified experimentally due to the extremely flexible nature of the matieral, i.e. its flexural stiffness is too low to measure in practice.

6. CONCLUSIONS

A general theory was developed for predicting the maximum bending moment that can be carried by beams having arbitrary compact cross sections and constructed of material having an arbitrary non-linear stress-strain curve that is different in tension and in compression. As an application of the theory, it was applied to rectangular-cross-section beams of plain concrete and of cord-rubber.

ACKNOWLEDGMENTS

The author acknowledges the financial support of the Office of Naval Research, Mechanics Division, and the continued encouragement of Drs. N. Basdekas and Y. Rajapakse.

APPENDIX A: RELATIONS BETWEEN TENSILE AND COMPRESSIVE STRENGTHS AND MATERIAL DAMAGE

1. Tension Loading

Using

$$\sigma = E\varepsilon + F_t\varepsilon^2 \quad ; \quad \varepsilon > 0 \tag{A1}$$

it is obvious that material instability cannot occur unless $F_t < 0$. Then the Considere criterion [12] is

$$\frac{d\sigma}{d\varepsilon} = 0 \tag{A2}$$

or

$$E + 2F_t\varepsilon = 0$$

Thus, the strain at which tensile instability occurs is

$$\varepsilon_{ti} = -E/2F_t \tag{A3}$$

and the tensile strength is

$$\sigma_{tu} = -\frac{E^2}{2F_t} + \frac{E^2}{4F_t} = -\frac{E^2}{4F_t} = D_t/4 \tag{A4}$$

2. Compression Loading

Using

$$\sigma = E\varepsilon + F_c\varepsilon^2 \quad ; \quad \varepsilon < 0 \tag{A5}$$

it is obvious that material instability cannot occur in this situation unless $F_c > 0$. Again using the Considère criterion, equation (A2), one obtains the following expression for the instabilty strain:

$$\varepsilon_{ci} = -E/2F_c \tag{A6}$$

and the predicted compressive strength is

$$\sigma_{cu} = -\frac{E^2}{2F_c} + \frac{E^2}{4F_c} = -E^2/4F_c = D_c/4 \qquad (A7)$$

APPENDIX B: EFFECT OF POWER-LAW TENSILE-DAMAGE FUNCTION ON BENDING STRENGTH OF CONCRETE

1. Bending Loading

In the continuum damage theory [17], the nominal stress σ is related to the net or true stress S by the following relation

$$\sigma = (1-\omega)S \qquad (B1)$$

Here ω is called the damage.

Piechnik and Pachla [30] proposed the following power-law damage function for concrete in tension:

$$\omega = (S/D_t)^n \qquad (B2)$$

Here n and D_t are material constants. Based on limited test data, Piechnik and Pachla recommended a value of 4 for n. Thus, the following expressions for ω are used here:

$$\omega = \begin{cases} (S/D_t)^n & \text{for } S > 0 \\ 0 & \text{for } S < 0 \end{cases} \qquad (B3)$$

Since

$$S = E\varepsilon \qquad (B4)$$

we obtain the following expression for the stress distribution

$$\sigma = \begin{cases} \sigma_c(E) = E\varepsilon & \varepsilon < 0 \\ \sigma_t(E) = E\varepsilon - E(E/D_t)^n\varepsilon^{n+1} & \varepsilon > 0 \end{cases} \qquad (B5)$$

It is readily apparent that this model is a generalization of the linear-damage model hypothesized by Krajcinovic [14].

Use of equation (B5) in equation (3) leads to the following relationship between the curvature κ and the dimensionless tensile-outer-fiber distance ($K_t \equiv C_t/H$):

$$\kappa = (D_t/EHK_t)[1+(n/2)]^{1/n}(2K_t^{-1} - K_t^{-2})^{1/n} \qquad (B6)$$

Similarly, substitution of equation (B5) into equation (5) and integration gives

$$3M/BE\kappa H^3 = K_t^3+(1-K_t)^3 - [3(2+n)/2(3+n)](2K_t^2-K_t) \quad (B7)$$

Finally, substitution of equation (B6) into equation (B7) yields

$$m = 6M/BD_tH^2 = 2[1+(n/2)]^{1/n}\,(2K_t^{-1}-K_t^{-2})^{1/n}[K_t^{-1}-3+N + (3-2N)K_t] \quad (B8)$$

Obviously, for the case of linear damage (n = 1), equation (B8) reduces to equation (13).

2. Tension Loading

Applying the tensile instability criterion, equation (A2) to $\sigma_t(E)$ as given by equation (B5), one obtains the following expressions for the instability strain and ultimate tensile strength:

$$\varepsilon_{ti} = (D_t/E)(n+1)^{-1/n} \quad (B9)$$

$$\sigma_{tu} = D(n+1)^{-1/n}[1-(n+1)^{-n+1}] \quad (B10)$$

Table 1. Effect of ratio of compressive to tensile strength on ratio of bending to tensile strength

f_{cu}/f_{tu}	F_c/F_t	f_{bu}/f_{tu}
∞	0	1.63
10	1/10	1.61
3	1/3	1.57

REFERENCES

1. B. Saint-Venant, Notes to the 3rd Edn. of Navier's *Résumé des leçons de la résistance des corps solides*, p. 175. Paris (1864).

2. G. N. J. Gilbert, Stress strain properties of cast iron and Poisson's ratio in tension and compression, *Brit. Cast Iron Res. Assn. J.* 9, 347-363 (1961).

3. S. K. Clark, The plane elastic characteristics of cord-rubber laminates, *Textile Res. J.* 33, 295-313 (1963).

4. I. P. Zemlyakov, On the difference in the moduli of elasticity of polyamides subjected to different kinds of deformation, *Polymer Mech.* 1, 25-27 (1965).

5. K. J. Seefried, H. Gesund, and G. Pincus, An experimental investigation of the strain distribution in the split cylinder test, *J. Matls.* 2, 703-718 (1967).

6. A. Simkin and G. Robin, The mechanical testing of bone in bending, *J. Biomech.* 6, 31-39 (1973).

7. B. C. Haimson and T. M. Tharp, Stresses around boreholes in bilinear elastic rock, *Soc. Petroleum Engrs J.* 14 (3), 145-151 (1974).

8. G. W. Pearsall and V. L. Roberts, Passive mechanical properties of uterine muscle (myometrium), *J. Biomech.* 11, 167-176 (1978).

9. C. Bach and R. Baumann, *Elastizität und Festigkeit*, 9th Edn., p. 259, Springer Verlag, Berlin (1914).

10. A. Nadai, *Theory of Flow and Fracture of Solids*, 2nd Edn., McGraw-Hill, New York (1950).

11. C. W. Bert, E. J. Mills, and W. S. Hyler, Effect of variation of Poisson's ratio on plastic tensile instability, *J. Basic Engrg., Trans. ASME* 89D, 35-39 (1967).

12. A. Considère, Memoir on the use of iron and steel in structures (in French), *Annales des Ponts et Chaussees*, ser. 6, 9, 574-775 (1885).

13. P.C. Bostrom, Damage induced instability in beam bending, *Int. J. Non-Linear Mech.* 11, 303-313 (1976).

14. D. Krajcinovic, Distributed damage theory of beams in pure bending, *J. Appl. Mech.* 46, 592-596 (1979).

15. J. Janson and J. Hult, Fracture mechanics and damage mechanics, a combined approach, *J. mécanique appliquée* 1, 69-84 (1977).

16. L. M. Kachanov, On the time to failure under creep conditions (in Russian), *Izv. Akad. Nauk, Otd. Tekh. Nauk* no. 8, 26-31 (1958).

17. J. Hult, CDM-capabilities, limitations and promises, *Mechanisms of Deformation and Fracture* (Proc. of a conference, Un . of Lulea, Sweden), K. E. Easterling, ed., Pergamon, Oxford, pp. 233-247 (1979).

18. The structural use of concrete, Brit. Std. CP110:1972, Brit. Standards Institution, London (1972).

19. C. W. Bert and M. Kumar, Experimental investigation of the mechanical behavior of cord-rubber materials, ONR Contract N00014-78-C-0647, Tech. Rept. No. 23, Univ. of Oklahoma, Norman (1981).

20. C. W. Bert and M. Kumar, discussion of Ref. [14], *J. Appl. Mech.* 47, 449-450 (1980).

21. H. Gonnerman and E. C. Shuman, Compression, flexure and tension tests of plain concrete, *Proc. ASTM* 28, 527-573 (1928).

22. J. J. Brooks and A. M. Neville, A comparison of creep, elasticity and strength of concrete in tension and in compression, *Magazine of Concrete Research* 29, 131-141 (1977).

23. M. A. Weil and I. M. Daniel, Analysis of fracture probabilities in nonuniformly stressed brittle materials, *J. Amer. Ceramic Soc.* 47, 268-274 (1964).

24. W. Weibull, A Statistical distribution function of wide applicability, *J. Appl. Mech.* 18, 293-297 (1951).

25. A. Ses. Jayatilaka, *Fracture of Engineering Brittle Materials*, Applied Science Publishers, London (1979).

26. T. T. C. Hsu, F. O. Slate, G. M. Sturman, and G. Winter, Microcracking of plain concrete and the shape of the stress-strain curve, *J. Amer. Concrete Inst., Proc.* 60, 209-224 (1963).

27. D. C. Spooner and J. W. Dougill, A quantitative assessment of damage sustained in concrete during compressive loading, *Magazine of Concrete Res.* 27, 151-160 (1975).

28. D. J. Spooner, J. D. Pomeroy, and J. W. Dougill, Damage and energy dissipation in cement pastes in compression, *Magazine of Concrete Res.* 28, 21-29 (1976).

29. J. W. Dougill, J. C. Lau, and N. J. Burt, Towards a theoretical model for progressive failure and softening in rock, concrete and similar materials, *Mechanics in Engineering*, Univ. of Waterloo Press, Waterloo, Ontario, Canada, pp. 335-355 (1977).

30. D. J. Cook and P. Chindaprasirt, A mathematical model for the prediction of damage in concrete, *Cement and Concrete Research* 11, 581-590 (1981).

31. S. Piechnik and H. Pachla, Law of continuous damage parameter for non-ageing materials, *Engng. Fract. Mech.* 12, 199-209 (1979).

32. W. H. Price, Factors influencing concrete strength, *J. Amer. Concrete Inst., Proc.* 47, 417-432 (1951).

33. A. T. Young, discussion of Ref. [26], *Magazine of Concrete Res.* 28, 108-109 (1976).

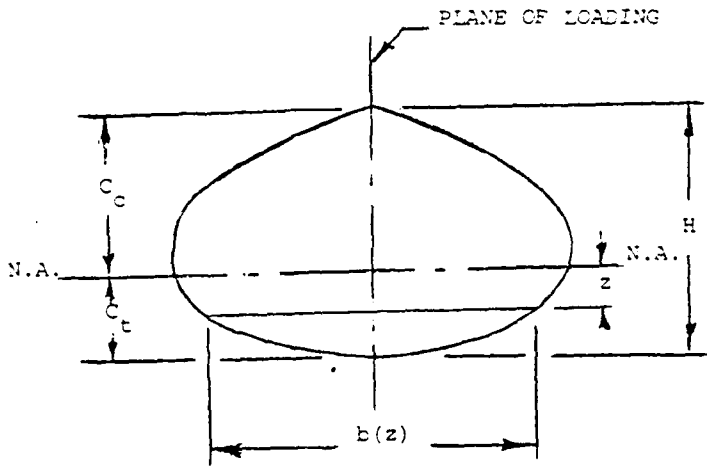

Fig. 1. Schematic diagram of arbitrary beam cross section with one axis of symmetry. The neutral axis is denoted by N.A.

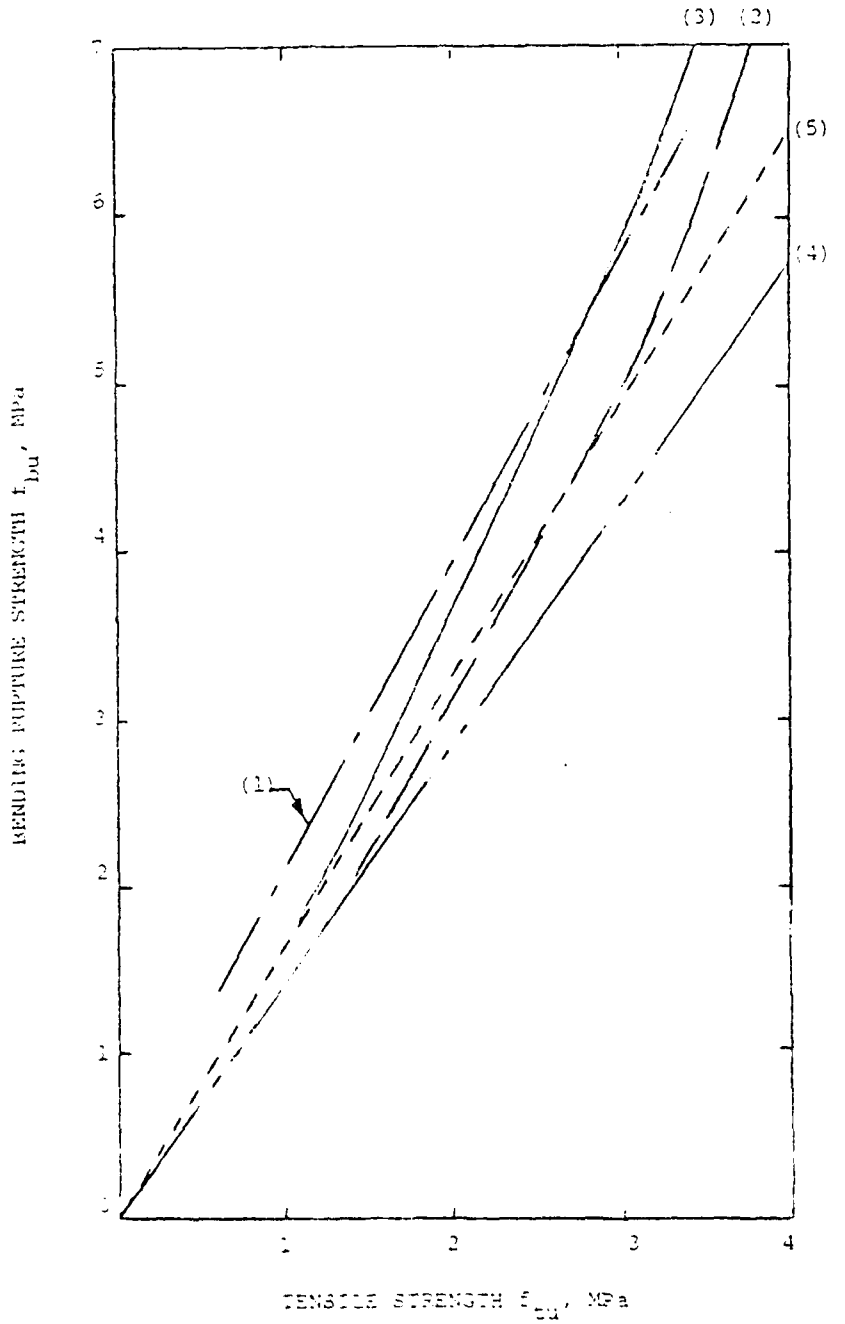

Fig. 1. Relation between bending rupture strength and tensile strength: (1) Ref. 11 experiments, (2) Ref. 10 (dry stored), (3) Ref. 10 (wet stored), (4) Ref. 14 theory, (5) Ref. 11 and present theory.

PREVIOUS REPORTS ON THIS CONTRACT

Project Rept. No.	Issuing University Rept. No.*	Report Title	Author(s)
1	OU 79-7	Mathematical Modeling and Micromechanics of Fiber Reinforced Bimodulus Composite Material	C.W. Bert
2	OU 79-8	Analyses of Plates Constructed of Fiber-Reinforced Bimodulus Materials	J.N. Reddy & C.W. Bert
3	OU 79-9	Finite-Element Analyses of Laminated Composite-Material Plates	J.N. Reddy
4A	OU-79-10A	Analyses of Laminated Bimodulus Composite-Material Plates	C.W. Bert
5	OU 79-11	Recent Research in Composite and Sandwich Plate Dynamics	C.W. Bert
6	OU 79-14	A Penalty Plate-Bending Element for the Analysis of Laminated Anisotropic Composite Plates	J.N. Reddy
7	OU 79-18	Finite-Element Analysis of Laminated Bimodulus Composite-Material Plates	J.N. Reddy & W.C. Chao
8	OU 79-19	A Comparison of Closed-Form and Finite-Element Solutions of Thick Laminated Anisotropic Rectangular Plates	J.N. Reddy
9	OU 79-20	Effects of Shear Deformation and Anisotropy on the Thermal Bending of Layered Composite Plates	J.N. Reddy & Y.S. Hsu
10	OU 80-1	Analyses of Cross-Ply Rectangular Plates of Bimodulus Composite Material	V.S. Reddy & C.W. Bert
11	OU 80-2	Analysis of Thick Rectangular Plates Laminated of Bimodulus Composite Materials	C.W. Bert, J.N. Reddy, V.S. Reddy, W.C. Chao
12	OU 80-3	Cylindrical Shells of Bimodulus Composite Material	C.W. Bert & V.S. Reddy
13	OU 80-6	Vibration of Composite Structures	C.W. Bert
14	OU 80-7	Large Deflection and Large-Amplitude Free Vibrations of Laminated Composite-Material Plates	J.N. Reddy & W.C. Chao
15	OU 80-8	Vibration of Thick Rectangular Plates of Bimodulus Composite Material	C.W. Bert, J.N. Reddy, W.C. Chao, & V.S. Reddy
16	OU 80-9	Thermal Bending of Thick Rectangular Plates of Bimodulus Material	J.N. Reddy, C.W. Bert, Y.S. Hsu, & V.S. Reddy
17	OU 80-14	Thermoelasticity of Circular Cylindrical Shells Laminated of Bimodulus Composite Materials	Y.S. Hsu, J.N. Reddy, & C.W. Bert
18	OU 30-17	Composite Materials: A Survey of the Damping Capacity of Fiber-Reinforced Composites	C.W. Bert
19	OU 80-20	Vibration of Cylindrical Shells of Bimodulus Composite Materials	C.W. Bert & M. Kumar
20	VPI 81-11 & OU 81-1	On the Behavior of Plates Laminated of Bimodulus Composite Materials	J.N. Reddy & C.W. Bert
21	VPI 81-12	Analysis of Layered Composite Plates Accounting for Large Deflections and Transverse Shear Strains	J.N. Reddy

*OU denotes the University of Oklahoma; VPI denotes Virginia Polytechnic Institute and State University.

Previous Reports on this Contract - Cont'd
Page 2

Project Rept. No.	Issuing University Rept. No.	Report Title	Author(s)
22	OU 81-7	Static and Dynamic Analyses of Thick Beams of Bimodular Materials	C.W. Bert & A.D. Tran
23	OU 81-8	Experimental Investigation of the Mechanical Behavior of Cord-Rubber Materials	C.W. Bert & M. Kumar
24	VPI 81.28	Transient Response of Laminated, Bimodular-Material Composite Rectangular Plates	J.N. Reddy
25	VPI 82.2	Nonlinear Bending of Bimodular-Material Plates	J.N. Reddy & W.C. Chao
26	OU 82-2	Analytical and Experimental Investigations of Bimodular Composite Beams	C.W. Bert, C.A. Rebello, & C.J. Rebello
27	OU 82-3	Research on Dynamics of Composite and Sandwich Plates, 1979-81	C.W. Bert
28	OU 82-4 & VPI 82.20	Mechanics of Bimodular Composite Structures	C.W. Bert & J.N. Reddy
29	VPI 82.19	Three-Dimensional Finite Element Analysis of Layered Composite Structures	W.C. Chao, N.S. Putcha, and J.N. Reddy

UNCLASSIFIED

SECURITY CLASSIFICATION OF THIS PAGE (When Data Entered)

REPORT DOCUMENTATION PAGE	READ INSTRUCTIONS BEFORE COMPLETING FORM
1. REPORT NUMBER: OU-AMNE-82-5	2. GOVT ACCESSION NO.: AD-A117944
	3. RECIPIENT'S CATALOG NUMBER:
4. TITLE (and Subtitle): ANALYSES OF BEAMS CONSTRUCTED OF NONLINEAR MATERIALS HAVING DIFFERENT BEHAVIOR IN TENSION AND COMPRESSION	5. TYPE OF REPORT & PERIOD COVERED: Technical Report No. 30
	6. PERFORMING ORG. REPORT NUMBER:
7. AUTHOR(s): C.W. Bert and F. Gordaninejad	8. CONTRACT OR GRANT NUMBER(s): N00014-78-C-0647
9. PERFORMING ORGANIZATION NAME AND ADDRESS: School of Aerospace, Mechanical and Nuclear Engineering, University of Oklahoma, Norman, OK 73019	10. PROGRAM ELEMENT, PROJECT, TASK AREA & WORK UNIT NUMBERS: NR 064-609
11. CONTROLLING OFFICE NAME AND ADDRESS: Department of the Navy, Office of Naval Research, Mechanics Division (Code 432), Arlington, Virginia 22217	12. REPORT DATE: July 1982
	13. NUMBER OF PAGES: 69
14. MONITORING AGENCY NAME & ADDRESS(if different from Controlling Office)	15. SECURITY CLASS. (of this report): UNCLASSIFIED
	15a. DECLASSIFICATION/DOWNGRADING SCHEDULE:

16. DISTRIBUTION STATEMENT (of this Report)

This document has been approved for public release and sale; distribution unlimited.

17. DISTRIBUTION STATEMENT (of the abstract entered in Block 20, if different from Report)

18. SUPPLEMENTARY NOTES

19. KEY WORDS (Continue on reverse side if necessary and identify by block number)

Beams, bending strength, bending-stretching coupling, bimodular materials, continuum damage mechanics, cord-rubber, multimodular materials, nonlinear materials, static bending, transfer-matrix method.

20. ABSTRACT (Continue on reverse side if necessary and identify by block number)

This report consists of two parts. In part I, a transfer-matrix analysis is presented for determining the static behavior of thick beams of "multimodular materials" (i.e., materials which have different elastic behavior in tension and compression, with nonlinear stress-strain curves approximated as piece-wise linear, with four or more segments). To validate the transfer-matrix method results, a closed-form solution is also presented for cases in which the neutral-surface location is constant along the beam axis. (over)

DD FORM 1 JAN 73 1473 EDITION OF 1 NOV 65 IS OBSOLETE S/N 0102-014-6601

UNCLASSIFIED

SECURITY CLASSIFICATION OF THIS PAGE (When Data Entered)

20. Abstract (cont'd)

Numerical results for axial displacement, transverse deflection, bending slope, bending moment, transverse shear, axial force, and location of neutral surface are presented for multimodular and bimodular models of unidirectional aramid cord-rubber. The transfer-matrix method results agree very well with the closed-form solutions.

In part II, it is shown by analysis that different behavior in tension and compression has a profound effect on the flexural strength as predicted by application of fundamental continuum mechanics relations. The theory is applied to a nonlinear material model which is shown to be applicable to two widely different materials: concrete, which has more strength degradation (modeled by continuum damage mechanics) in tension than in compression, and steel cord-rubber, which has strength which is enhanced in tension by cord strengthening and degraded in compression by cord microbuckling.


DATE
FILME
8